The colored Jones polynomials as vortex partition functions

Masahide Manabe,[a,1] **Seiji Terashima**[b] **and Yuji Terashima**[c]

[a]*School of Mathematics and Statistics, University of Melbourne,*
Royal Parade, Parkville, VIC 3010, Australia

[b]*Yukawa Institute for Theoretical Physics, Kyoto University,*
Kyoto 606-8502, Japan

[c]*Graduate School of Science, Tohoku University,*
Aramaki-aza-Aoba 6-3, Aoba-ku, Sendai, 980-8578, Japan

E-mail: masahidemanabe@gmail.com, terasima@yukawa.kyoto-u.ac.jp,
yujiterashima@tohoku.ac.jp

ABSTRACT: We construct 3D $\mathcal{N} = 2$ abelian gauge theories on $\mathbb{S}^2 \times \mathbb{S}^1$ labeled by knot diagrams whose K-theoretic vortex partition functions, each of which is a building block of twisted indices, give the colored Jones polynomials of knots in $\mathbb{S}^3$. The colored Jones polynomials are obtained as the Wilson loop expectation values along knots in SU(2) Chern-Simons gauge theories on $\mathbb{S}^3$, and then our construction provides an explicit correspondence between 3D $\mathcal{N} = 2$ abelian gauge theories and 3D SU(2) Chern-Simons gauge theories. We verify, in particular, the applicability of our constructions to a class of tangle diagrams of 2-bridge knots with certain specific twists.

---

[1]Affiliated until December 2020 to: School of Mathematics and Statistics, University of Melbourne, Royal Parade, Parkville, VIC 3010, Australia.

Contents

1 Introduction

In supersymmetric quantum field theories, recent localization techniques enable us to obtain various exact results which are made accessible to researchers for understanding or proposing conjectural dualities and for providing various mathematical conjectures, etc. See e.g. [1] for a review and references therein. In this paper, we focus on the A-twisted partition function of 3D $\mathcal{N} = 2$ gauge theory on $\mathbb{S}^2 \times_q \mathbb{S}^1$, with the Ω-deformation parameter $\hbar = -\log q$, known as the twisted index and obtained exactly by Benini and Zaffaroni

in [2], where the twisted partition function is factorized into the K-theoretic vortex partition functions which are considered as the partition functions on $\mathbb{D}^2 \times_q \mathbb{S}^1$ with appropriate boundary conditions [2–11].

The main object of this paper is to construct 3D $\mathcal{N} = 2$ abelian gauge theories $T[\mathcal{K}]$ for knots $\mathcal{K}$, and show that the colored Jones polynomials of $\mathcal{K}$ in $\mathbb{S}^3$, which can be understood as the Wilson loop expectation values along $\mathcal{K}$ in SU(2) Chern-Simons gauge theories on $\mathbb{S}^3$ [12], are obtained as the K-theoretic vortex partition functions of $T[\mathcal{K}]$. Therefore, our construction gives a new correspondence between 3D $\mathcal{N} = 2$ abelian gauge theories and 3D SU(2) Chern-Simons gauge theories:

vortex partition function of $T[\mathcal{K}]$ = Wilson loop along $\mathcal{K}$ in SU(2) Chern-Simons theory.

This reminds of the 3D-3D correspondence [4, 13–19] (see also [20]) which is a 3D-3D analogue of the Alday-Gaiotto-Tachikawa (4D-2D) correspondence [21, 22], and says that the compactification of the 6D (2,0) theory of type A_1 twisted along a 3-manifold M_3 implies that a 3D $\mathcal{N} = 2$ abelian gauge theory $T[M_3]$ labeled by M_3 is related to a 3D SL$(2, \mathbb{C})$ Chern-Simons gauge theory on M_3.[1] Remark that our correspondence treats Wilson loops in SU(2) Chern-Simons theories which are more manageable than SL$(2, \mathbb{C})$ Chern-Simons theories.

More specifically, we propose how the colored Jones polynomials of knots, associated with the quantum group $U_q(\mathfrak{sl}_2)$, are constructed as K-theoretic vortex partition functions, obtained from a factorization of the twisted indices of abelian gauge theories on $\mathbb{S}^2 \times_q \mathbb{S}^1$, where the deformation parameter q of $U_q(\mathfrak{sl}_2)$ is identified with the Ω-deformation parameter. Our strategy is to construct the building blocks of the colored Jones polynomial, given by the R-matrix etc. assigned to a tangle diagram of a knot [23] (see [24] for a survey), as building blocks of a K-theoretic vortex partition function. Then, for any knot diagram, we systematically associate a matter content and Chern-Simons couplings in 3D $\mathcal{N} = 2$ abelian gauge theory whose K-theoretic vortex partition function, in a certain specific limit, gives the colored Jones polynomial of the knot. In this paper, we refer to the gauge theories $T[\mathcal{K}]$ labeled by knot diagrams as *knot-gauge theories.* Here, for a knot, one can consider infinitely many tangles, related by the Reidemeister moves I, II and III, which provide the same colored Jones polynomial of the knot. As a result, for a knot $\mathcal{K}$, we have infinitely many 3D $\mathcal{N} = 2$ gauge theories $T[\mathcal{K}]$ that are hopefully related to one another by some 3D dualities.

The localization formula in [2] of the A-twisted partition function is written as a middle-dimensional contour integral, in the space parametrized by the complex scalars (the real scalars in the vector multiplet and the holonomies of the gauge fields along $\mathbb{S}^1$), which is organized as the Jeffrey-Kirwan (JK) residue [25] (see also [26–28]). The JK residue depends on the choice of a vector (stability parameters), and the most technical part of our gauge theory constructions is how to choose the vector. In this paper, we show that there exists a choice of the vectors which gives identifications between K-theoretic vortex

---

[1]Although the relation between the gauge theories $T[\mathcal{K}]$ in this paper and the gauge theories $T[M_3]$ in the context of the 3D-3D correspondence is not clear, we use the same notation $T[\mathcal{K}]$ to denote our gauge theories.

partition functions and the colored Jones polynomials for a class of tangle diagrams of 2-bridge knots with certain specific twists. We expect that, by a refinement of the choice, the identifications are also established for any knot diagram.[2]

It is expected that the K-theoretic vortex partition function of $T[\mathcal{K}]$ is interpreted as a generating function of Euler characteristics for moduli spaces of vortices [10, 11, 29, 30]. Under our correspondence, it implies that we have a new geometric interpretation of the colored Jones polynomial. This will be an interesting mathematical and physical problem.

This paper is organized as follows. In section 2, the A-twisted partition function (twisted index) of 3D $\mathcal{N} = 2$ gauge theory on $\mathbb{S}^2 \times_q \mathbb{S}^1$ in [2] is recalled, and then the factorization into the K-theoretic vortex partition functions is provided. In section 3, we first construct elementary constituents of knot-gauge theories which correspond to the building blocks of the colored Jones polynomials of knots as R-matrix. We then construct the knot-gauge theories $T[\mathcal{K}]$, and discuss the JK residue procedure in detail. In particular, we show Proposition 3.10 for a class of 2-bridge knots, and exemplify the trefoil knot as well as the unknot. In section 4, we construct yet another but simpler abelian gauge theories $T^{\mathrm{red}}[\mathcal{K}]$ labeled by knot diagrams referred to as *reduced knot-gauge theories*, and exemplify the trefoil knot, the figure-eight knot and the 3-twist knot. In appendix A, properties of the q-Pochhammer symbol are summarized.

2 K-theoretic vortex partition function

In this section, we first recall the A-twisted partition function of 3D $\mathcal{N} = 2$ gauge theory on $\mathbb{S}^2 \times_q \mathbb{S}^1$ in [2], with the Ω-deformation parameter $\hbar = -\log q$, and then provide the building blocks of K-theoretic vortex partition function by factorizing the twisted partition function.[3]

2.1 Twisted partition function on $\mathbb{S}^2 \times_q \mathbb{S}^1$

Consider a topologically twisted 3D $\mathcal{N} = 2$ gauge theory on $\mathbb{S}^2 \times_q \mathbb{S}^1$ which consists of vector multiplet V with rank($\mathfrak{g}$) Lie algebra $\mathfrak{g}$ of a gauge group G and N chiral multiplets $\Phi_{\mathfrak{R}_i}^{\mathsf{r}_i}$, $i = 1, \ldots, N$, with representation $\mathfrak{R}_i$ of $\mathfrak{g}$, $\mathrm{U}(1)_R$ charge $\mathsf{r}_i \in \mathbb{Z}$, and (complexified) mass $\gamma_i = \boldsymbol{U}_f^{\rho_{f,i}}$, where $\boldsymbol{U}_f$ are the (complexified) holonomies (the real masses and the holonomies of the background gauge fields along $\mathbb{S}^1$) associated with a global symmetry G_f and $\rho_{f,i}$ are the flavor weights.[4] In [2], by the supersymmetric localization [1], the A-twisted partition function of the 3D gauge theory is obtained and written in terms of the

---

[2]The full twisted index with the boundary contribution in (2.3) should not depend on the stability vector. In this paper, we ignore the boundary contribution by assuming that it is irrelevant to the vortex partition functions obtained for our choice of stability parameters. If the stability parameters are changed, the boundary contribution would need to be taken into account for obtaining the colored Jones polynomials. This is a subtle point, and it may be interesting to investigate other choices of the stability vectors in the knot-gauge theories.

[3]The $\mathcal{N} = 2$ superconformal index on $\mathbb{S}^2 \times_q \mathbb{S}^1$ without the topological twist [31–33] also enjoys the similar factorization [5].

[4]Although, for 3D-3D correspondence discussed in this paper, it is enough to consider the cases with abelian symmetries, we will not assume it in this section.

following building blocks associated with the vector multiplet V and each chiral multiplet $\Phi_{\mathfrak{R}}^{\mathsf{r}}$ of mass γ as

$$\widehat{\mathcal{Z}}_{\boldsymbol{d}}^{V}(\boldsymbol{U};q) = \left(-q^{-\frac{1}{2}}\right)^{\sum_{\alpha\in\Delta_+}\alpha(\boldsymbol{d})} \prod_{\alpha\in\Delta_+} \left(1 - \boldsymbol{U}^{-\alpha}q^{\frac{1}{2}\alpha(\boldsymbol{d})}\right)\left(1 - \boldsymbol{U}^{\alpha}q^{\frac{1}{2}\alpha(\boldsymbol{d})}\right), \qquad (2.1)$$

$$\widehat{\mathcal{Z}}_{\boldsymbol{d}}^{\Phi_{\mathfrak{R}}^{\mathsf{r}}}(\boldsymbol{U};\gamma,q) = \prod_{\rho\in\mathfrak{R}} \frac{(\gamma\boldsymbol{U}^{\rho})^{\frac{\rho(\boldsymbol{d})+1-\mathsf{r}}{2}}}{\left(\gamma\boldsymbol{U}^{\rho}q^{\frac{\mathsf{r}-\rho(\boldsymbol{d})}{2}};q\right)_{\rho(\boldsymbol{d})+1-\mathsf{r}}}, \qquad (2.2)$$

where Δ_+ is the set of positive roots of $\mathfrak{g}$, $\alpha(*)$ and $\rho(*)$ are the canonical pairings, and $\boldsymbol{U} = (U_1,\ldots,U_{\mathrm{rank}(\mathfrak{g})})$, $U_a = \mathrm{e}^{-u_a}$, $\boldsymbol{U}^{\alpha} = \mathrm{e}^{-\alpha(\boldsymbol{u})}$, $\boldsymbol{U}^{\rho} = \mathrm{e}^{-\rho(\boldsymbol{u})}$. Here $\boldsymbol{u} = (u_1,\ldots,u_{\mathrm{rank}(\mathfrak{g})})$, $u_a \in \mathfrak{h}\otimes_{\mathbb{R}}\mathbb{C}$, are the complex scalars (the real scalars in the vector multiplet V and the holonomies of the gauge fields along $\mathbb{S}^1$), where $\mathfrak{h}$ is the Cartan subalgebra of $\mathfrak{g}$. These building blocks are indexed by the magnetic fluxes $\boldsymbol{d} = (d_1,\ldots,d_{\mathrm{rank}(\mathfrak{g})})$, $d_a \in \mathbb{Z}$, associated with $\mathrm{U}(1)^{\mathrm{rank}(\mathfrak{g})}(\subset G)$ gauge fields on $\mathbb{S}^2$. The q-Pochhammer symbol $(x;q)_d$ is defined in (A.1). When the gauge group contains central $\mathrm{U}(1)^{\mathsf{c}} \subset G$ factors, the gauge theories admit deformations with the 3D complexified Fayet-Iliopoulos (FI) parameters τ^a, $a = 1,\ldots,\mathsf{c}$. Then the A-twisted partition function on $\mathbb{S}^2 \times_q \mathbb{S}^1$ without Chern-Simons factors (see Remark 2.1 for Chern-Simons factors) is given by [2]

$$Z_{\mathbb{S}^2\times_q\mathbb{S}^1}(\boldsymbol{z},\boldsymbol{\gamma},q) = \frac{1}{|\mathcal{W}|} \sum_{\boldsymbol{d}\in\mathbb{Z}^{\mathrm{rank}(\mathfrak{g})}} \oint_{\Gamma} d^{\mathrm{rank}(\mathfrak{g})}u\, \widehat{\mathcal{Z}}_{\boldsymbol{d}}^{\mathrm{total}}(\boldsymbol{U};\boldsymbol{z},\boldsymbol{\gamma},q) + \text{boundary contribution},$$

$$\widehat{\mathcal{Z}}_{\boldsymbol{d}}^{\mathrm{total}}(\boldsymbol{U};\boldsymbol{z},\boldsymbol{\gamma},q) := \boldsymbol{z}^{\boldsymbol{d}}\, \widehat{\mathcal{Z}}_{\boldsymbol{d}}^{V}(\boldsymbol{U};q) \prod_{i=1}^{N} \widehat{\mathcal{Z}}_{\boldsymbol{d}}^{\Phi_{\mathfrak{R}_i}^{\mathsf{r}_i}}(\boldsymbol{U};\gamma_i,q). \qquad (2.3)$$

Here $|\mathcal{W}|$ is the order of the Weyl group of G, and $\boldsymbol{z}^{\boldsymbol{d}} = \mathrm{e}^{2\pi\mathrm{i}\,\tau(\boldsymbol{d})}$, where the pairing $\tau(\boldsymbol{d}) = \sum_a \tau^a d_a$ is defined by the embedding $\boldsymbol{\tau} \hookrightarrow \mathfrak{h}^*\otimes_{\mathbb{R}}\mathbb{C}$. The middle-dimensional contour integral along Γ is defined by the JK residue [25] (see also [26–28]) which picks up relevant poles in $\widehat{\mathcal{Z}}_{\boldsymbol{d}}^{\Phi_{\mathfrak{R}_i}^{\mathsf{r}_i}}$ depending on the choice of a vector (stability parameters). In this paper, for simplicity we identify the stability parameters with the FI parameters $\xi_a = \mathrm{Im}(\tau^a)$ (see [28] for the difference between them). Although the partition function has a boundary contribution at $u_a = \pm\infty$, we assume that the boundary contribution is irrelevant to the vortex partition functions in this paper and only focus on the bulk (first) factor (see [34] for an interpretation of the boundary contribution as *topological saddles* of an effective supersymmetric quantum mechanics).

Note that, the background magnetic fluxes $\boldsymbol{d}_f$ associated with the global symmetry G_f are also introduced by the shifts in (2.2) as

$$\rho(\boldsymbol{d}) \to \rho(\boldsymbol{d}) + d_{f,i}, \qquad d_{f,i} = \rho_{f,i}(\boldsymbol{d}_f). \qquad (2.4)$$

Remark 2.1. Assume that the gauge symmetry G to be abelian (or consider abelian factors in G). The gauge/flavor-gauge/flavor/R Chern-Simons factors associated with G

and G_f are introduced by [2, 35, 36] (see also [37])

$$\widehat{\mathcal{Z}}_{\boldsymbol{d}}^{\text{g-g}}(\boldsymbol{U};\boldsymbol{k}) = \prod_{a,b} U_a^{k_{ab} d_b}, \quad \widehat{\mathcal{Z}}_{\boldsymbol{d},\boldsymbol{d}_f}^{\text{g-f}}(\boldsymbol{U};\boldsymbol{\gamma},\boldsymbol{k}^{\text{g-f}}) = \prod_{i,a} \left(\gamma_i^{d_a} U_a^{d_{f,i}} \right)^{k_{ai}^{\text{g-f}}}, \tag{2.5}$$

$$\widehat{\mathcal{Z}}_{\boldsymbol{d}_f}^{\text{f-f}}(\boldsymbol{\gamma},\boldsymbol{k}^{\text{f-f}}) = \prod_{i,j} \gamma_i^{k_{ij}^{\text{f-f}} d_{f,j}}, \qquad \widehat{\mathcal{Z}}^{\text{g-R}}(\boldsymbol{U};\boldsymbol{k}^{\text{g-R}}) = \prod_{a} U_a^{k_a^{\text{g-R}}}, \qquad\qquad \widehat{\mathcal{Z}}^{\text{f-R}}(\boldsymbol{\gamma},\boldsymbol{k}^{\text{f-R}}) = \prod_{i} \gamma_i^{k_i^{\text{f-R}}}.$$

Here $\boldsymbol{k}$, $\boldsymbol{k}^{\text{g-f}}$, $\boldsymbol{k}^{\text{f-f}}$, $\boldsymbol{k}^{\text{g-R}}$ and $\boldsymbol{k}^{\text{f-R}}$ are, respectively, the set of relevant Chern-Simons couplings $k_{ab} = k_{ba}$, $k_{ai}^{\text{g-f}}$, $k_{ij}^{\text{f-f}} = k_{ji}^{\text{f-f}}$, $k_a^{\text{g-R}}$ and $k_i^{\text{f-R}}$.

2.2 K-theoretic vortex partition function by factorization

Let us recall how the A-twisted partition function is factorized into K-theoretic vortex partition functions [2, 9–11]. For a choice of FI parameters, the contour Γ in (2.3) encloses the poles in $\widehat{\mathcal{Z}}_{\boldsymbol{d}}^{\Phi_{\mathfrak{R}}^{\mathsf{r}}}$, with the inclusion of the background magnetic fluxes by (2.4), as

$$\gamma \boldsymbol{U}^{\rho} = q^{-\frac{1}{2}\rho(\boldsymbol{d}) + \frac{1}{2}\mathsf{r} + p}, \quad p = -\frac{1}{2}\rho_f(\boldsymbol{d}_f), -\frac{1}{2}\rho_f(\boldsymbol{d}_f) + 1, \ldots, \rho(\boldsymbol{d}) + \frac{1}{2}\rho_f(\boldsymbol{d}_f) - \mathsf{r}, \tag{2.6}$$

with $\rho(\boldsymbol{d}) + \rho_f(\boldsymbol{d}_f) - \mathsf{r} \geq 0$. By a change of variables

$$U_a = q^{\frac{d_a' - d_a''}{2}} \sigma_a, \qquad \boldsymbol{d} = \boldsymbol{d}' + \boldsymbol{d}'', \qquad \gamma = q^{\frac{\rho_f(\boldsymbol{d}_f') - \rho_f(\boldsymbol{d}_f'')}{2}} \widetilde{\gamma}, \qquad \boldsymbol{d}_f = \boldsymbol{d}_f' + \boldsymbol{d}_f'', \tag{2.7}$$

with $\rho(\boldsymbol{d}') = p + \mathsf{r}/2 - \rho_f(\boldsymbol{d}_f')/2 + \rho_f(\boldsymbol{d}_f'')/2$, the poles (2.6) yield

$$\widetilde{\gamma}\boldsymbol{\sigma}^{\rho} = 1, \tag{2.8}$$

and the sum over the magnetic fluxes and the integration in (2.3) for $\Phi_{\mathfrak{R}}^{\mathsf{r}}$ are written as

$$\sum_{\rho(\boldsymbol{d}) + \rho_f(\boldsymbol{d}_f) \geq \mathsf{r}} \sum_{p=-\frac{1}{2}\rho_f(\boldsymbol{d}_f)}^{\rho(\boldsymbol{d}) + \frac{1}{2}\rho_f(\boldsymbol{d}_f) - \mathsf{r}} \oint_{\gamma \boldsymbol{U}^{\rho} = q^{-\frac{1}{2}\rho(\boldsymbol{d}) + \frac{1}{2}\mathsf{r} + p}} = \sum_{\rho(\boldsymbol{d}) + \rho_f(\boldsymbol{d}_f) \geq \mathsf{r}} \sum_{\rho(\boldsymbol{d}') = \frac{\mathsf{r}}{2} - \rho_f(\boldsymbol{d}_f')}^{\rho(\boldsymbol{d}) + \rho_f(\boldsymbol{d}_f'') - \frac{\mathsf{r}}{2}} \oint_{\gamma \boldsymbol{\sigma}^{\rho} = 1}$$

$$= \sum_{\rho(\boldsymbol{d}') + \rho_f(\boldsymbol{d}_f'), \rho(\boldsymbol{d}'') + \rho_f(\boldsymbol{d}_f'') \geq \frac{\mathsf{r}}{2}} \oint_{\gamma \boldsymbol{\sigma}^{\rho} = 1}. \tag{2.9}$$

Here, we can take $\boldsymbol{d}_f'$ as an arbitrary integer satisfying $0 \leq \boldsymbol{d}_f' \leq \boldsymbol{d}_f$. Because the twisted index and the discussion below do not depend on this choice, we will take, for simplicity, $\boldsymbol{d}_f' = \boldsymbol{d}_f''$ below, and then $\widetilde{\gamma} = \gamma$. Under the reparametrization (2.7), by using $(x;q)_d = \left(q^{d-1}x; q^{-1} \right)_d$ in (A.2) and $(x;q)_{d_1+d_2} = (x;q)_{d_1} \left(q^{d_1}x; q \right)_{d_2}$ in (A.3), the building blocks (2.1) and (2.2) are factorized, respectively, as

$$\widehat{\mathcal{Z}}_{\boldsymbol{d}}^{V}(\boldsymbol{U};q) = I_{1\text{-loop}}^{V}(\boldsymbol{\sigma}) \, I_{\boldsymbol{d}'}^{V}(\boldsymbol{\sigma};q) \, I_{\boldsymbol{d}''}^{V}(\boldsymbol{\sigma};q^{-1}), \tag{2.10}$$

where

$$I_{1\text{-loop}}^{V}(\boldsymbol{\sigma}) = \prod_{\alpha \in \Delta_+} (-1) \left(\boldsymbol{\sigma}^{\frac{\alpha}{2}} - \boldsymbol{\sigma}^{-\frac{\alpha}{2}} \right)^2,$$

$$I_{\boldsymbol{d}}^{V}(\boldsymbol{\sigma};q) = \prod_{\alpha \in \Delta_+} \left(-q^{-\frac{1}{2}} \right)^{\alpha(\boldsymbol{d})} \frac{1 - \boldsymbol{\sigma}^{\alpha} q^{\alpha(\boldsymbol{d})}}{1 - \boldsymbol{\sigma}^{\alpha}} = \prod_{\alpha \in \Delta_+} \left(-q^{-\frac{1}{2}} \right)^{\alpha(\boldsymbol{d})} \frac{(q\boldsymbol{\sigma}^{\alpha};q)_{\alpha(\boldsymbol{d})}}{(\boldsymbol{\sigma}^{\alpha};q)_{\alpha(\boldsymbol{d})}}, \tag{2.11}$$

and

$$\widehat{\mathcal{Z}}_{\boldsymbol{d}}^{\Phi_{\mathfrak{R}}^{\mathsf{r}}}(\boldsymbol{U};\gamma,q) = I_{\text{1-loop}}^{\Phi_{\mathfrak{R}}^{\mathsf{r}}}(\boldsymbol{\sigma};\gamma,q)\,I_{\boldsymbol{d}'}^{\Phi_{\mathfrak{R}}^{\mathsf{r}}}(\boldsymbol{\sigma};\gamma,q)\,I_{\boldsymbol{d}''}^{\Phi_{\mathfrak{R}}^{\mathsf{r}}}(\boldsymbol{\sigma};\gamma,q^{-1}), \tag{2.12}$$

where

$$I_{\text{1-loop}}^{\Phi_{\mathfrak{R}}^{\mathsf{r}}}(\boldsymbol{\sigma};\gamma,q) = \prod_{\rho\in\mathfrak{R}} \frac{(\gamma\boldsymbol{\sigma}^{\rho})^{\frac{1-\mathsf{r}}{2}}}{\left(\gamma\boldsymbol{\sigma}^{\rho}q^{\frac{\mathsf{r}}{2}};q\right)_{1-\mathsf{r}}},$$

$$I_{\boldsymbol{d}}^{\Phi_{\mathfrak{R}}^{\mathsf{r}}}(\boldsymbol{\sigma};\gamma,q) = \prod_{\rho\in\mathfrak{R}} \frac{q^{\frac{1}{4}\rho(\boldsymbol{d})(\rho(\boldsymbol{d})+1-\mathsf{r})}\,(\gamma\boldsymbol{\sigma}^{\rho})^{\frac{1}{2}\rho(\boldsymbol{d})}}{\left(\gamma\boldsymbol{\sigma}^{\rho}q^{1-\frac{\mathsf{r}}{2}};q\right)_{\rho(\boldsymbol{d})}}, \tag{2.13}$$

and the background magnetic fluxes are now introduced by the similar shift to (2.4) (i.e. $\rho(\boldsymbol{d})\to\rho(\boldsymbol{d})+2\rho_f(\boldsymbol{d}_f)$ for $\widehat{\mathcal{Z}}_{\boldsymbol{d}}^{\Phi_{\mathfrak{R}}^{\mathsf{r}}}$ and $\rho(\boldsymbol{d})\to\rho(\boldsymbol{d})+\rho_f(\boldsymbol{d}_f)$ for $I_{\boldsymbol{d}}^{\Phi_{\mathfrak{R}}^{\mathsf{r}}}$). The twisted partition function (2.3) is then factorized into

$$I_{\text{1-loop}}(\boldsymbol{\sigma};\boldsymbol{\gamma},q) = I_{\text{1-loop}}^V(\boldsymbol{\sigma})\prod_{i=1}^{N} I_{\text{1-loop}}^{\Phi_{\mathfrak{R}_i}^{\mathsf{r}_i}}(\boldsymbol{\sigma};\gamma_i,q), \tag{2.14}$$

and the K-theoretic vortex partition function

$$I_{\text{vortex}}(\boldsymbol{\sigma};\boldsymbol{z},\boldsymbol{\gamma},q) = \sum_{\boldsymbol{d}} I_{\boldsymbol{d}}(\boldsymbol{\sigma};\boldsymbol{z},\boldsymbol{\gamma},q) = \sum_{\boldsymbol{d}} \boldsymbol{z}^{\boldsymbol{d}}\,I_{\boldsymbol{d}}^V(\boldsymbol{\sigma};q)\prod_{i=1}^{N} I_{\boldsymbol{d}}^{\Phi_{\mathfrak{R}_i}^{\mathsf{r}_i}}(\boldsymbol{\sigma};\gamma_i,q), \tag{2.15}$$

as [2, 9–11] (see also [7, 8])[5]

$$Z_{\mathbb{S}^2\times_q\mathbb{S}^1}(\boldsymbol{z},\boldsymbol{\gamma},q) \sim \sum_{\boldsymbol{\sigma}^*} I_{\text{1-loop}}(\boldsymbol{\sigma}^*;\boldsymbol{\gamma},q)\,I_{\text{vortex}}(\boldsymbol{\sigma}^*;\boldsymbol{z},\boldsymbol{\gamma},q)\,I_{\text{vortex}}(\boldsymbol{\sigma}^*;\boldsymbol{z},\boldsymbol{\gamma},q^{-1}), \tag{2.16}$$

up to an overall normalization and the boundary contribution, where the shift (2.4) for each $I_{\boldsymbol{d}}^{\Phi_{\mathfrak{R}_i}^{\mathsf{r}_i}}$ introduces background magnetic fluxes. Here the domain of $\boldsymbol{d}$ is determined as (2.9) for a choice of the FI parameters. The domain of $\boldsymbol{\sigma}^* = \boldsymbol{\sigma}(\boldsymbol{\gamma})$ is determined as well. Note that when $\rho(\boldsymbol{d}) > 0$, the poles (2.8) for an $\mathsf{r} = 0$ chiral multiplet $\Phi_{\mathfrak{R}}^0$ are in the "1-loop factor" $I_{\text{1-loop}}^{\Phi_{\mathfrak{R}}^0}$ for $\mathsf{r} = 0$, whereas the poles (2.8) for an $\mathsf{r} = 2$ chiral multiplet $\Phi_{\mathfrak{R}}^2$ are in the "vortex factor" $I_{\boldsymbol{d}}^{\Phi_{\mathfrak{R}}^2}$ for $\mathsf{r} = 2$ (one zeros from $I_{\text{1-loop}}^{\Phi_{\mathfrak{R}}^2}$ and two poles from $I_{\boldsymbol{d}'}^{\Phi_{\mathfrak{R}}^2}$ and $I_{\boldsymbol{d}''}^{\Phi_{\mathfrak{R}}^2}$ in (2.12)).

Remark 2.2. By (A.2), the factors in (2.13) are rewritten as

$$I_{\text{1-loop}}^{\Phi_{\mathfrak{R}}^{\mathsf{r}}}(\boldsymbol{\sigma};\gamma,q) = \prod_{\rho\in\mathfrak{R}} (-1)^{1-\mathsf{r}}\,(\gamma\boldsymbol{\sigma}^{\rho})^{-\frac{1-\mathsf{r}}{2}}\left(\gamma^{-1}\boldsymbol{\sigma}^{-\rho}q^{1-\frac{\mathsf{r}}{2}};q\right)_{\mathsf{r}-1},$$

$$I_{\boldsymbol{d}}^{\Phi_{\mathfrak{R}}^{\mathsf{r}}}(\boldsymbol{\sigma};\gamma,q) = \prod_{\rho\in\mathfrak{R}} (-1)^{\rho(\boldsymbol{d})}q^{-\frac{1}{4}\rho(\boldsymbol{d})(\rho(\boldsymbol{d})+1-\mathsf{r})}\,(\gamma\boldsymbol{\sigma}^{\rho})^{-\frac{1}{2}\rho(\boldsymbol{d})}\left(\gamma^{-1}\boldsymbol{\sigma}^{-\rho}q^{\frac{\mathsf{r}}{2}};q\right)_{-\rho(\boldsymbol{d})}, \tag{2.17}$$

where $\boldsymbol{\sigma}^{-1} = (\sigma_1^{-1},\dots,\sigma_{\text{rank}(\mathfrak{g})}^{-1})$.

---

[5]The factorization into the "1-loop factor" and the "vortex factor" has ambiguities, and so it is desirable to prescribe how to fix them. A decomposition of $\mathbb{S}^2\times_q\mathbb{S}^1$ into two $\mathbb{D}^2\times_q\mathbb{S}^1$ is known to lead to the factorization [5], and the partition functions on $\mathbb{D}^2\times_q\mathbb{S}^1$ with appropriate boundary conditions are expected to unambiguously provide the K-theoretic vortex partition functions [38–40].

Remark 2.3. Similarly, we factorize the Chern-Simons factors in (2.5) as

$$
\begin{aligned}
\widehat{\mathcal{Z}}_{\boldsymbol{d}}^{\text{g-g}}(\boldsymbol{U};\boldsymbol{k}) &= I_{\boldsymbol{d'}}^{\text{g-g}}(\boldsymbol{\sigma};q,\boldsymbol{k})\, I_{\boldsymbol{d''}}^{\text{g-g}}(\boldsymbol{\sigma};q^{-1},\boldsymbol{k}), \\
\widehat{\mathcal{Z}}_{\boldsymbol{d},2\boldsymbol{d}_f}^{\text{g-f}}(\boldsymbol{U};\boldsymbol{\gamma},\boldsymbol{k}^{\text{g-f}}) &= I_{\boldsymbol{d'},\boldsymbol{d}_f}^{\text{g-f}}(\boldsymbol{\sigma};\boldsymbol{\gamma},q,\boldsymbol{k}^{\text{g-f}})\, I_{\boldsymbol{d''},\boldsymbol{d}_f}^{\text{g-f}}(\boldsymbol{\sigma};\boldsymbol{\gamma},q^{-1},\boldsymbol{k}^{\text{g-f}}), \\
\widehat{\mathcal{Z}}_{2\boldsymbol{d}_f}^{\text{f-f}}(\boldsymbol{\gamma},\boldsymbol{k}^{\text{f-f}}) &= I_{\boldsymbol{d}_f}^{\text{f-f}}(q,\boldsymbol{k}^{\text{f-f}})\, I_{\boldsymbol{d}_f}^{\text{f-f}}(q^{-1},\boldsymbol{k}^{\text{f-f}}), \\
\widehat{\mathcal{Z}}^{\text{g-R}}(\boldsymbol{U};\boldsymbol{k}^{\text{g-R}}) &= I_{\text{1-loop}}^{\text{g-R}}(\boldsymbol{\sigma};\boldsymbol{k}^{\text{g-R}})\, I_{\boldsymbol{d'}}^{\text{g-R}}(q,\boldsymbol{k}^{\text{g-R}})\, I_{\boldsymbol{d''}}^{\text{g-R}}(q^{-1},\boldsymbol{k}^{\text{g-R}}), \\
\widehat{\mathcal{Z}}^{\text{f-R}}(\boldsymbol{\gamma},\boldsymbol{k}^{\text{f-R}}) &= I_{\text{1-loop}}^{\text{f-R}}(\boldsymbol{\gamma},\boldsymbol{k}^{\text{f-R}})\, I_{\boldsymbol{d}_f}^{\text{f-R}}(q,\boldsymbol{k}^{\text{f-R}})\, I_{\boldsymbol{d}_f}^{\text{f-R}}(q^{-1},\boldsymbol{k}^{\text{f-R}}),
\end{aligned}
\tag{2.18}
$$

where

$$
I_{\text{1-loop}}^{\text{g-R}}(\boldsymbol{\sigma};\boldsymbol{k}^{\text{g-R}}) = \prod_a \sigma_a^{k_a^{\text{g-R}}}, \quad I_{\text{1-loop}}^{\text{f-R}}(\boldsymbol{\gamma},\boldsymbol{k}^{\text{f-R}}) = \prod_i \gamma_i^{k_i^{\text{f-R}}},
\tag{2.19}
$$

are considered to be normalization (1-loop) factors which are irrelevant to d_a and $d_{f,i}$, and

$$
I_{\boldsymbol{d}}^{\text{g-g}}(\boldsymbol{\sigma};q,\boldsymbol{k}) = \prod_{a,b}\left(\sigma_a^{d_b} q^{\frac{1}{2}d_a d_b}\right)^{k_{ab}}, \qquad I_{\boldsymbol{d},\boldsymbol{d}_f}^{\text{g-f}}(\boldsymbol{\sigma};\boldsymbol{\gamma},q,\boldsymbol{k}^{\text{g-f}}) = \prod_{i,a}\left(\gamma_i^{d_a}\sigma_a^{d_{f,i}} q^{d_{f,i}d_a}\right)^{k_{ai}^{\text{g-f}}},
$$

$$
I_{\boldsymbol{d}_f}^{\text{f-f}}(q,\boldsymbol{k}^{\text{f-f}}) = \prod_{i,j}\left(\gamma_i^{d_{f,j}} q^{\frac{1}{2}d_{f,i}d_{f,j}}\right)^{k_{ij}^{\text{f-f}}},
$$

$$
I_{\boldsymbol{d}}^{\text{g-R}}(q,\boldsymbol{k}^{\text{g-R}}) = \prod_a q^{\frac{1}{2}k_a^{\text{g-R}}d_a}, \qquad\qquad I_{\boldsymbol{d}_f}^{\text{f-R}}(q,\boldsymbol{k}^{\text{f-R}}) = \prod_i q^{\frac{1}{2}k_i^{\text{f-R}}d_{f,i}}.
\tag{2.20}
$$

Here the background magnetic fluxes are taken to be $2\boldsymbol{d}_f$ for the factorizations of the mass parameters γ_i as $\gamma_i = q^{(d_{f,i}-d_{f,i})/2}\gamma_i$ following (2.7) with $\boldsymbol{d}_f' = \boldsymbol{d}_f''$.

3 Knot-gauge theory

We construct 3D $\mathcal{N}=2$ abelian gauge theories labeled by knot diagrams, referred to as knot-gauge theories, whose K-theoretic vortex partition functions give the colored Jones polynomials of knots. For that purpose, we first recall how the colored Jones polynomials are obtained for tangle diagrams of knots from elementary building blocks as R-matrix, and, in section 3.2, construct corresponding constituents of knot-gauge theories for the elementary building blocks. We then discuss the JK residue procedure in the knot-gauge theories, and in particular show that, for a class of knot diagrams in Proposition 3.10, the K-theoretic vortex partition functions actually give the colored Jones polynomials.

3.1 A brief summary of colored Jones polynomials from tangles

Let us recall the building blocks R, R^{-1}, μ and μ^{-1}, associated with the quantum group $U_q(\mathfrak{sl}_2)$, which give the n-colored Jones polynomials of knots colored by symmetric representations S^n [23] (see also [24]). The $(n+1)^2 \times (n+1)^2$ R-matrix $R = R(q)$ for n-colored Jones polynomial of a knot $\mathcal{K}$, assigned to each positive crossing in a tangle diagram of $\mathcal{K}$,

is given by [41]

$$R_{d_{42}d_{34}}^{d_{12}d_{31}} =$$

$$= (-1)^{d_{31}-d_{42}} q^{\frac{1}{2}(d_{31}-d_{42})(d_{31}-d_{42}-1)+d_{42}d_{34}-\frac{1}{2}n(d_{31}+d_{34})+\frac{1}{4}n^2}$$

$$\times \frac{(q)_{n-d_{42}}(q)_{d_{34}}}{(q)_{d_{12}}(q)_{n-d_{31}}(q)_{d_{31}-d_{42}}}, \tag{3.1}$$

where $(q)_d = (q;q)_d$. Here, following [42], the variables d_i, $i = 1, 2, 3, 4$, are assigned to regions around the crossing, $d_{ij} = d_i - d_j$ are assigned to arcs, and

$$d_{12}, \quad d_{31}, \quad d_{42}, \quad d_{34}, \quad d_{31} - d_{42} \in \{0, 1, \ldots, n\}. \tag{3.2}$$

For the variables d_i that do not satisfy the conditions (3.2), $R_{d_{42}d_{34}}^{d_{12}d_{31}} = 0$ is defined. Note that the arrows in (3.1) are promised to be in the downward directions (see (4.10) for local deformations of tangle). The inverse R-matrix $R^{-1} = R(q)^{-1}$, assigned to each negative crossing, is similarly given by

$$\left(R^{-1}\right)_{d_{42}d_{34}}^{d_{12}d_{31}} =$$

$$= R(q^{-1})_{d_{34}d_{42}}^{d_{31}d_{12}}$$

$$= q^{-d_{12}d_{31}+\frac{1}{2}n(d_{31}+d_{34})-\frac{1}{4}n^2} \frac{(q)_{d_{42}}(q)_{n-d_{34}}}{(q)_{n-d_{12}}(q)_{d_{31}}(q)_{d_{12}-d_{34}}}, \tag{3.3}$$

where

$$d_{12}, \quad d_{31}, \quad d_{42}, \quad d_{34}, \quad d_{12} - d_{34} \in \{0, 1, \ldots, n\}. \tag{3.4}$$

To each local minimum and maximum in the tangle diagram

$$\mu_{d_{12}} = \quad \overset{d_{12}\ \ d_1}{\underset{d_2}{\curvearrowright}} \quad = q^{d_{12}-\frac{1}{2}n},$$

$$\mu_{d_{12}}^{-1} = \quad \overset{d_1}{\underset{d_2\ \ d_{12}}{\curvearrowright}} \quad = q^{-d_{12}+\frac{1}{2}n}, \tag{3.5}$$

are assigned, respectively, where $0 \le d_{12} \le n$. We also set

$$\overset{d_{12}\ \ d_2}{\underset{d_1}{\curvearrowright}} \quad = \quad \overset{d_2}{\underset{d_1\ \ d_{12}}{\curvearrowright}} \quad = 1. \tag{3.6}$$

Using the above building blocks, the n-colored Jones polynomial of a knot $\mathcal{K}$ is given by

$$\overline{J}_n^{\mathcal{K}}(q) = \sum_{\boldsymbol{d}} \left(\prod_{i \in P(\boldsymbol{d})} q^{-\frac{1}{4}n(n+2)} R_i \right) \left(\prod_{i \in N(\boldsymbol{d})} q^{\frac{1}{4}n(n+2)} R_i^{-1} \right) \left(\prod_{i \in \min(\boldsymbol{d})} \mu_i \right) \left(\prod_{i \in \max(\boldsymbol{d})} \mu_i^{-1} \right). \tag{3.7}$$

Here, for a $(0,0)$-tangle (the closure of a $(1,1)$-tangle) diagram of $\mathcal{K}$, $P(\boldsymbol{d})$, $N(\boldsymbol{d})$, $\min(\boldsymbol{d})$ and $\max(\boldsymbol{d})$ are the set of positive crossings, negative crossings, local minima and local maxima with the variables $\boldsymbol{d}$, respectively, and R_i, R_i^{-1}, μ_i and μ_i^{-1} denote the i-th R-matrix, the i-th inverse R-matrix, the quantity assigned to the i-th local minimum and the quantity assigned to the i-th local maximum, respectively. The domain of $\boldsymbol{d}$ is determined for the given $(0,0)$-tangle diagram of $\mathcal{K}$ by (3.2) and (3.4). The normalized colored Jones polynomial is also introduced by

$$J_n^{\mathcal{K}}(q) = \frac{\overline{J}_n^{\mathcal{K}}(q)}{\overline{J}_n^{\boldsymbol{0}}(q)}, \tag{3.8}$$

where

$$\overline{J}_n^{\boldsymbol{0}}(q) = \sum_{d=0}^{n} \bigcirc\!\!\!\!\!d \;=\; \sum_{d=0}^{n} \mu_d = \frac{q^{\frac{1}{2}(n+1)} - q^{-\frac{1}{2}(n+1)}}{q^{\frac{1}{2}} - q^{-\frac{1}{2}}} = q^{-\frac{1}{2}n} \frac{(q^2; q)_n}{(q; q)_n}, \tag{3.9}$$

is the (unnormalized) colored Jones polynomial of unknot. The normalized colored Jones polynomial is shown to be given for the $(1,1)$-tangle diagram of $\mathcal{K}$ [41, Lemma 3.9] (see also [24, section 2.5]) with an incoming (outgoing) constant $f \in \{0, 1, \ldots, n\}$ assigned to the external arcs as in figure 1, which specifies a basis of the vector space attached to the tangle diagram,

$$J_n^{\mathcal{K}}(q) = \sum_{\boldsymbol{d}} \left(\prod_{i \in P(\boldsymbol{d}, f)} q^{-\frac{1}{4}n(n+2)} R_i \right) \left(\prod_{i \in N(\boldsymbol{d}, f)} q^{\frac{1}{4}n(n+2)} R_i^{-1} \right)$$
$$\times \left(\prod_{i \in \min(\boldsymbol{d}, f)} \mu_i \right) \left(\prod_{i \in \max(\boldsymbol{d}, f)} \mu_i^{-1} \right). \tag{3.10}$$

Remark that the normalized colored Jones polynomial does not depend on the constant f.

3.2 Building blocks of knot-gauge theories

We recalled that the normalized colored Jones polynomials are obtained from the building blocks R, R^{-1}, μ and μ^{-1} by (3.10). Based on the formulation, we propose a construction of 3D $\mathcal{N} = 2$ abelian gauge theories labeled by $(1,1)$-tangle diagrams.

Consider a $(1,1)$-tangle diagram of a knot $\mathcal{K}$ with the number of loops (regions) N_v and an incoming (outgoing) constant $f \in \{0, 1, \ldots, n\}$ (see figure 1 for an example of $N_v = 3$). We assign variables d_I, $I = 0, 1, \ldots, N_v$, to the bounded and unbounded regions, and take $d_0 = 0$ without loss of generality by a shift of variables. By associating a $\mathrm{U}(1)_I$ gauge symmetry to the region with the non-zero variable d_I, we construct a $\mathrm{U}(1)^{N_v} =$
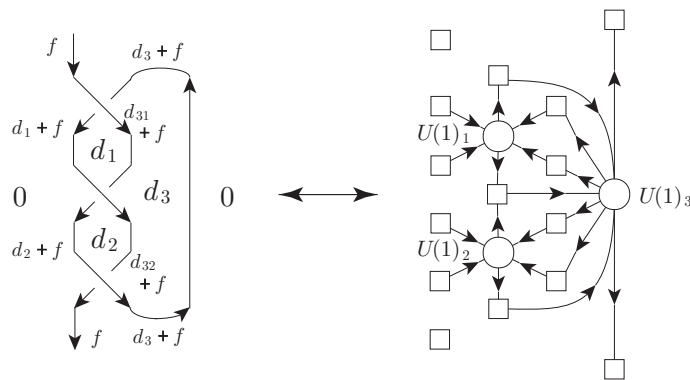
Figure 1. The left figure is a $(1,1)$-tangle diagram of the trefoil knot $\mathbf{3_1}$, and the right figure, which is obtained by the associations as in figure 2 for all the crossings, represents the associated quiver-like diagram of $U(1)^3$ gauge theory $T[\mathbf{3_1}]$ with 15 chiral fields (in table 3) and extra Chern-Simons couplings. The variables d_1, d_2, d_3 are assigned to the bounded regions, and an incoming (outgoing) constant $f \in \{0, 1, \ldots, n\}$ is identified with the background magnetic flux for the global symmetry $U(1)_{ext}$.
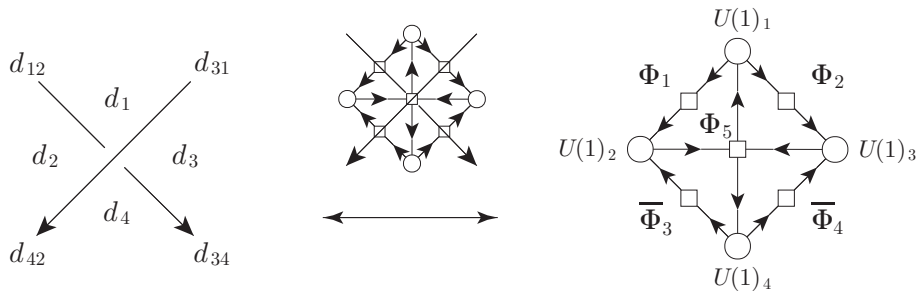
Figure 2. For the R-matrix, the quiver-like diagram on the right is associated, where the circles represent the $U(1)_i$ gauge nodes and the squares denote five chiral fields given in table 1. The same applies to the inverse R-matrix in section 3.2.2.

$U(1)_1 \times \cdots \times U(1)_{N_v}$ gauge theory $T[\mathcal{K}]$, where the variables d_I are identified with the magnetic fluxes. Here the number of crossings is also N_v, and a matter content for the R- or inverse R-matrix assigned at each crossing is constructed in the following, where each matter content provides a building block of the 3D $\mathcal{N} = 2$ $U(1)^{N_v}$ gauge theory $T[\mathcal{K}]$, that we call the knot-gauge theory. We will see that the knot-gauge theory has a global symmetry $U(1)_F^{2N_v}$, and the color n and the constant f are, respectively, identified with the background magnetic fluxes for global symmetries $U(1)_c$ and $U(1)_{ext}$ in $U(1)_F^{2N_v}$:

$$U(1)_c, \ U(1)_{ext} \subset U(1)_F^{2N_v}. \tag{3.11}$$

In the following, we construct the building blocks of $T[\mathcal{K}]$. Once they are constructed, it is straightforward to construct the gauge theory $T[\mathcal{K}]$ from them.

3.2.1 R-matrix

We focus on a crossing, with an assigned R-matrix, for a $(1,1)$-tangle diagram with N_v crossings. Let $U(1)_i$, $i = 1, 2, 3, 4$, be gauge symmetries with associated complex scalars σ_i

Field	$U(1)_1$	$U(1)_2$	$U(1)_3$	$U(1)_4$	$U(1)_c$	$U(1)_{ext}$	mass	$U(1)_R$
Φ_1	1	-1	0	0	0	1	γ_1	0
Φ_2	1	0	-1	0	1	-1	γ_2	0
$\overline{\Phi}_3$	0	-1	0	1	-1	1	γ_2^{-1}	2
$\overline{\Phi}_4$	0	0	-1	1	0	-1	γ_1^{-1}	2
Φ_5	-1	1	1	-1	0	0	1	0

Table 1. Matter content for the R-matrix $R_{d_{42}d_{34}}^{d_{12}d_{31}}$ in (3.1) which is denoted by $T[R_{d_{42}d_{34}}^{d_{12}d_{31}}(\boldsymbol{\gamma})]$ including extra Chern-Simons couplings (3.16), where $U(1)_R$ denotes the $U(1)_R$ charge.

and magnetic fluxes d_i, and associate the quiver-like diagram of figure 2 with the five chiral fields (multiplets) in table 1. Here, note that the gauge symmetries act, in general, on not only the chiral fields at the crossing but also the chiral fields at other crossings which share the same regions in the tangle diagram. The chiral fields interact through a superpotential $W = \Phi_1 \overline{\Phi}_4 \Phi_5 + \Phi_2 \overline{\Phi}_3 \Phi_5$ (see also Remark 3.1), and two mass parameters $\boldsymbol{\gamma} = (\gamma_1, \gamma_2)$, associated with a global symmetry $U(1)_F^2$, are introduced. Overall, $2N_v$ mass parameters, associated with a global symmetry $U(1)_F^{2N_v}$, are introduced for the tangle diagram, and the global symmetries $U(1)_c$ and $U(1)_{ext}$, which associates non-negative background magnetic fluxes $2n$ and $2f$, are two of $U(1)_F^{2N_v}$ as (3.11). Note that the $3N_v$ $U(1)$ symmetries associated with the $5N_v$ chiral multiplets with the superpotential are generated by $U(1)^{N_v}$ gauge symmetries and $U(1)_F^{2N_v}$ flavor symmetries. We now construct the R-matrix (3.1) as a building block of K-theoretic vortex partition functions.

From (2.13) and (2.17), the five chiral fields lead to a 1-loop building block

$$I_{1\text{-loop}}^R(\boldsymbol{\sigma}; \boldsymbol{\gamma}) = \left(\frac{\sigma_1 \sigma_4}{\sigma_2 \sigma_3}\right)^{\frac{1}{2}} \frac{\left(1 - \gamma_2 \frac{\sigma_2}{\sigma_4}\right)\left(1 - \gamma_1 \frac{\sigma_3}{\sigma_4}\right)}{\left(1 - \gamma_1 \frac{\sigma_1}{\sigma_2}\right)\left(1 - \gamma_2 \frac{\sigma_1}{\sigma_3}\right)\left(1 - \frac{\sigma_2 \sigma_3}{\sigma_1 \sigma_4}\right)}, \tag{3.12}$$

and a building block of K-theoretic vortex partition functions

$$I_{\boldsymbol{d},n,f}^R(\boldsymbol{\sigma}; \boldsymbol{\gamma}, q) = (-1)^{d_{23}+n} \, q^{\frac{1}{4}(d_{12}-d_{34})(3d_1 - d_2 - d_3 - d_4 + 2n + 1)} \, (\gamma_1 \gamma_2)^{\frac{1}{2}(d_{12}-d_{34})}$$

$$\times \left(\frac{\sigma_1^3 \sigma_4}{\sigma_2^2 \sigma_3^2}\right)^{\frac{1}{2}d_1} \left(\frac{\sigma_2 \sigma_3}{\sigma_1^2}\right)^{\frac{1}{2}(d_2+d_3)} \left(\frac{\sigma_1}{\sigma_4}\right)^{\frac{1}{2}d_4} \left(\frac{\sigma_1 \sigma_4}{\sigma_2 \sigma_3}\right)^{\frac{1}{2}n}$$

$$\times \frac{\left(q\gamma_2 \frac{\sigma_2}{\sigma_4}; q\right)_{n-d_{42}-f} \left(q\gamma_1 \frac{\sigma_3}{\sigma_4}; q\right)_{d_{34}+f}}{\left(q\gamma_1 \frac{\sigma_1}{\sigma_2}; q\right)_{d_{12}+f} \left(q\gamma_2 \frac{\sigma_1}{\sigma_3}; q\right)_{n-d_{31}-f} \left(q\frac{\sigma_2 \sigma_3}{\sigma_1 \sigma_4}; q\right)_{d_{31}-d_{42}}}, \tag{3.13}$$

where $\boldsymbol{\sigma} = (\sigma_1, \sigma_2, \sigma_3, \sigma_4)$, $d_{ij} = d_i - d_j$, and the background magnetic fluxes n and f for the global symmetries $U(1)_c$ and $U(1)_{ext}$ are introduced by the shift (2.4). In addition to the matter content in table 1 we also introduce Chern-Simons couplings by (2.19) and (2.20) as

$$I_{1\text{-loop}}^{\text{CS}}(\boldsymbol{\sigma}) = \left(\frac{\sigma_1 \sigma_4}{\sigma_2 \sigma_3}\right)^{\frac{1}{2}}, \tag{3.14}$$

and

$$I^{\mathrm{CS}}_{\boldsymbol{d},n,f}(\boldsymbol{\sigma};q) = q^{-\frac{1}{4}(d_1^2-d_2^2-d_3^2+d_4^2)+\frac{1}{2}(d_1d_4-d_2d_3+nd_{23})+\frac{1}{4}(d_{12}-d_{34})-\frac{1}{2}n+f^2-d_{23}f-nf}$$
$$\times \left(\frac{\sigma_4}{\sigma_1}\right)^{\frac{1}{2}d_{14}} \left(\frac{\sigma_2}{\sigma_3}\right)^{\frac{1}{2}d_{23}+\frac{1}{2}n-f}, \tag{3.15}$$

for non-zero Chern-Simons couplings

$$k_{11}= k_{44} = k_{23} = k_{32} = -\frac{1}{2}, \qquad k_{22} = k_{33} = k_{14} = k_{41} = \frac{1}{2},$$

$$k_{2c}^{\mathrm{g\text{-}f}} = \frac{1}{2}, \qquad k_{3c}^{\mathrm{g\text{-}f}} = -\frac{1}{2}, \qquad k_{2f}^{\mathrm{g\text{-}f}} = -1, \qquad k_{3f}^{\mathrm{g\text{-}f}} = 1,$$

$$k_1^{\mathrm{g\text{-}R}} = k_4^{\mathrm{g\text{-}R}} = \frac{1}{2}, \qquad k_2^{\mathrm{g\text{-}R}} = k_3^{\mathrm{g\text{-}R}} = -\frac{1}{2}, \qquad k_c^{\mathrm{f\text{-}R}} = -1, \qquad k_{cf}^{\mathrm{f\text{-}f}} = k_{fc}^{\mathrm{f\text{-}f}} = -1, \qquad k_{ff}^{\mathrm{f\text{-}f}} = 2, \tag{3.16}$$

where the subscripts i, c and f denote the indices for the gauge symmetries $\mathrm{U}(1)_i$, the global symmetries $\mathrm{U}(1)_c$ and $\mathrm{U}(1)_{ext}$, respectively, and the mass parameters for $\mathrm{U}(1)_c$ and $\mathrm{U}(1)_{ext}$ are abbreviated. By combining the block (3.13) with the Chern-Simons factor (3.15), we define a building block for the R-matrix:

$$I^{T[R^{d_{12}d_{31}}_{d_{42}d_{34}}(\boldsymbol{\gamma})]}_{n,f}(\boldsymbol{\sigma};q) := (-1)^n\, I^{\mathrm{CS}}_{\boldsymbol{d},n,f}(\boldsymbol{\sigma};q)\, I^{R}_{\boldsymbol{d},n,f}(\boldsymbol{\sigma};\boldsymbol{\gamma},q), \tag{3.17}$$

where the label $T[R^{d_{12}d_{31}}_{d_{42}d_{34}}(\boldsymbol{\gamma})]$ is introduced.[6] If the complex scalars are specialized as

$$\sigma_1,\sigma_2,\sigma_3,\sigma_4 \to 1, \tag{3.18}$$

then under massless limit

$$\gamma_1,\gamma_2 \to 1, \tag{3.19}$$

the building block (3.17) yields the R-matrix (3.1) with the constant shift f:

$$(-1)^{d_{14}}\, I^{T[R^{d_{12}d_{31}}_{d_{42}d_{34}}(\boldsymbol{\gamma})]}_{n,f}(\boldsymbol{\sigma};q) \quad \to \quad q^{-\frac{1}{4}n(n+2)}\, R^{d_{12}+f\ d_{31}+f}_{d_{42}+f\ d_{34}+f}. \tag{3.20}$$

Here the prefactor $(-1)^{d_{14}}$ on the left side is introduced by specializing the complexified FI parameters, and the prefactor $q^{-n(n+2)/4}$ on the right side corresponds to a normalization factor appeared in (3.10). The conditions (3.2) for the magnetic fluxes and the specializations (3.18) of the complex scalars should be obtained by means of the JK residue in (2.3) for a choice of the FI parameters. In section 3.3 we will discuss the justification of these.

---

[6]The building block

$$I^{\mathrm{CS}}_{1\text{-loop}}(\boldsymbol{\sigma})\, I^R_{1\text{-loop}}(\boldsymbol{\sigma};\boldsymbol{\gamma})\big(I^{\mathrm{CS}}_{\boldsymbol{d'},n,f}(\boldsymbol{\sigma};q)\, I^R_{\boldsymbol{d'},n,f}(\boldsymbol{\sigma};\boldsymbol{\gamma},q)\big)\big(I^{\mathrm{CS}}_{\boldsymbol{d''},n,f}(\boldsymbol{\sigma};q^{-1})\, I^R_{\boldsymbol{d''},n,f}(\boldsymbol{\sigma};\boldsymbol{\gamma},q^{-1})\big)$$

of twisted partition functions, or table 1 with the Chern-Simons couplings (3.16), shows the absence of the parity anomalies except for the $\mathrm{U}(1)_1$-$\mathrm{U}(1)_c$ and $\mathrm{U}(1)_4$-$\mathrm{U}(1)_c$ parity anomalies. These parity anomalies just exist for each crossing, and one can show that they are canceled out for each loop in (1,1)-tangle diagrams and actually absent. Here, in general, the $\mathrm{U}(1)_a$-$\mathrm{U}(1)_b$ parity anomalies are absent when $k_{ab} + N/2$ is integer-valued, where k_{ab} is the $\mathrm{U}(1)_a$-$\mathrm{U}(1)_b$ Chern-Simons coupling and N is the number of chirals charged under both $\mathrm{U}(1)_a$ and $\mathrm{U}(1)_b$.
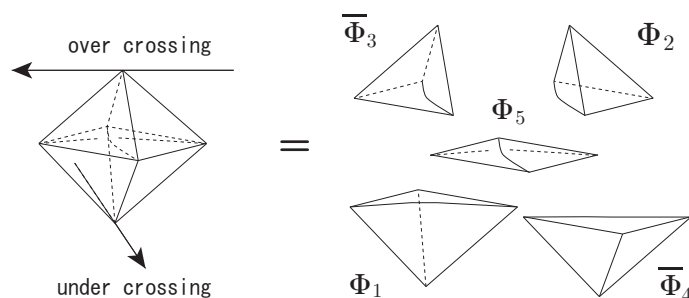
Figure 3. Geometric interpretation of the R-matrix by D. Thurston [43]. An octahedron is associated for the R-matrix and decomposed into five tetrahedra which correspond to the five chiral fields in table 1.

The non-trivial degenerate R-matrices

$$R_{d_{42}d_{34}}^{0\ d_{32}} = (-1)^{d_{34}} q^{\frac{1}{2}d_{34}(d_{32}+d_{42}-1)-\frac{1}{2}n(d_{32}+d_{34})+\frac{1}{4}n^2} \frac{(q)_{n-d_{42}}}{(q)_{n-d_{32}}}, \tag{3.21}$$

$$R_{0\ d_{32}}^{d_{12}d_{31}} = (-1)^{d_{31}} q^{\frac{1}{2}d_{31}(d_{31}-1)-\frac{1}{2}n(d_{31}+d_{32})+\frac{1}{4}n^2} \frac{(q)_n\,(q)_{d_{32}}}{(q)_{d_{12}}\,(q)_{n-d_{31}}\,(q)_{d_{31}}}, \tag{3.22}$$

$$R_{0\ d_{12}}^{d_{12}\ 0} = R_{d_{12}\ 0}^{0\ d_{12}} = q^{-\frac{1}{2}nd_{12}+\frac{1}{4}n^2}, \tag{3.23}$$

can be also constructed by identifying some U(1) gauge symmetries, by identifying U(1)$_1$ with U(1)$_2$ for (3.21) and by identifying U(1)$_4$ with U(1)$_3$ for (3.22). Here, by identifying U(1)$_1$ with U(1)$_2$, the U(1)$_1 \times$ U(1)$_2$ charges (a_1, a_2) of a chiral field are changed to the U(1)$_2$ charge $a_1 + a_2$. For the degenerate R-matrix (3.23), which is used in section 4, we will construct it just as a Chern-Simons factor as (4.2).

Remark 3.1. Following D. Thurston, to each crossing, with an assigned R-matrix, an octahedron, which can be decomposed into five tetrahedra, is attached (see figure 3) [43]. This provides a geometric interpretation of the R-matrix and is utilized to prove the volume conjecture [44, 45] for some specific hyperbolic knots in [46, 47]. In our gauge theory construction, each decomposed tetrahedron corresponds to a chiral field in table 1 or 2 (see [16] for a similar gauge theory construction of the octahedron by Dimofte, Gaiotto and Gukov).

3.2.2 Inverse R-matrix

For the inverse R-matrix (3.3), we consider the mater content in table 2 with mass parameters $\boldsymbol{\gamma} = (\gamma_1, \gamma_2)$ associated with a global symmetry U(1)$_F^2$. The chiral fields interact through a superpotential $W = \Phi_1' \overline{\Phi}_4' \Phi_5' + \Phi_2' \overline{\Phi}_3' \Phi_5'$. The associated building blocks of the 1-loop factors and the K-theoretic vortex partition functions are, respectively, given by

$$I_{\text{1-loop}}^{\overline{R}}(\boldsymbol{\sigma}; \boldsymbol{\gamma}) = \left(\frac{\sigma_2 \sigma_3}{\sigma_1 \sigma_4}\right)^{\frac{1}{2}} \frac{\left(1 - \gamma_2 \frac{\sigma_4}{\sigma_2}\right)\left(1 - \gamma_1 \frac{\sigma_4}{\sigma_3}\right)}{\left(1 - \gamma_1 \frac{\sigma_2}{\sigma_1}\right)\left(1 - \gamma_2 \frac{\sigma_3}{\sigma_1}\right)\left(1 - \frac{\sigma_1 \sigma_4}{\sigma_2 \sigma_3}\right)}, \tag{3.24}$$

Field	$U(1)_1$	$U(1)_2$	$U(1)_3$	$U(1)_4$	$U(1)_c$	$U(1)_{ext}$	mass	$U(1)_R$
Φ'_1	-1	1	0	0	1	-1	γ_1	0
Φ'_2	-1	0	1	0	0	1	γ_2	0
$\overline{\Phi}'_3$	0	1	0	-1	0	-1	γ_2^{-1}	2
$\overline{\Phi}'_4$	0	0	1	-1	-1	1	γ_1^{-1}	2
Φ'_5	1	-1	-1	1	0	0	1	0

Table 2. Matter content for the inverse R-matrix $\left(R^{-1}\right)^{d_{12}d_{31}}_{d_{42}d_{34}}$ in (3.3) which is denoted by $T[\overline{R}^{d_{12}d_{31}}_{d_{42}d_{34}}(\boldsymbol{\gamma})]$ including extra Chern-Simons couplings (3.28).

and

$$I^{\overline{R}}_{\boldsymbol{d},n,f}(\boldsymbol{\sigma};\boldsymbol{\gamma},q) = (-1)^{d_{23}+n} \, q^{\frac{1}{4}(d_{12}-d_{34})(3d_1-d_2-d_3-d_4-2n-1)} \left(\gamma_1\gamma_2\right)^{-\frac{1}{2}(d_{12}-d_{34})}$$

$$\times \left(\frac{\sigma_1^3\sigma_4}{\sigma_2^2\sigma_3^2}\right)^{\frac{1}{2}d_1} \left(\frac{\sigma_2\sigma_3}{\sigma_1^2}\right)^{\frac{1}{2}(d_2+d_3)} \left(\frac{\sigma_1}{\sigma_4}\right)^{\frac{1}{2}d_4} \left(\frac{\sigma_2\sigma_3}{\sigma_1\sigma_4}\right)^{\frac{1}{2}n}$$

$$\times \frac{\left(q\gamma_2\frac{\sigma_4}{\sigma_2};q\right)_{d_{42}+f}\left(q\gamma_1\frac{\sigma_4}{\sigma_3};q\right)_{n-d_{34}-f}}{\left(q\gamma_1\frac{\sigma_2}{\sigma_1};q\right)_{n-d_{12}-f}\left(q\gamma_2\frac{\sigma_3}{\sigma_1};q\right)_{d_{31}+f}\left(q\frac{\sigma_1\sigma_4}{\sigma_2\sigma_3};q\right)_{d_{12}-d_{34}}}. \tag{3.25}$$

By combining this block with Chern-Simons factors

$$I^{\overline{CS}}_{\text{1-loop}}(\boldsymbol{\sigma}) = \left(\frac{\sigma_1\sigma_4}{\sigma_2\sigma_3}\right)^{\frac{1}{2}}, \tag{3.26}$$

and

$$I^{\overline{CS}}_{\boldsymbol{d},n,f}(\boldsymbol{\sigma};q) = q^{\frac{1}{4}(d_1^2-d_2^2-d_3^2+d_4^2)-\frac{1}{2}(d_1d_4-d_2d_3+nd_{23})+\frac{1}{4}(d_{12}-d_{34})+\frac{1}{2}n-f^2+d_{23}f+nf}$$

$$\times \left(\frac{\sigma_1}{\sigma_4}\right)^{\frac{1}{2}d_{14}} \left(\frac{\sigma_3}{\sigma_2}\right)^{\frac{1}{2}d_{23}+\frac{1}{2}n-f}, \tag{3.27}$$

for non-zero Chern-Simons couplings

$$k_{11}= k_{44} = k_{23} = k_{32} = \frac{1}{2}, \qquad\qquad k_{22} = k_{33} = k_{14} = k_{41} = -\frac{1}{2},$$

$$k_{2c}^{\text{g-f}} = -\frac{1}{2}, \qquad k_{3c}^{\text{g-f}} = \frac{1}{2}, \qquad k_{2f}^{\text{g-f}} = 1, \quad k_{3f}^{\text{g-f}} = -1,$$

$$k_1^{\text{g-R}} = k_4^{\text{g-R}} = \frac{1}{2}, \qquad k_2^{\text{g-R}} = k_3^{\text{g-R}} = -\frac{1}{2}, \quad k_c^{\text{f-R}} = 1, \quad k_{cf}^{\text{f-f}} = k_{fc}^{\text{f-f}} = 1, \qquad k_{ff}^{\text{f-f}} = -2, \tag{3.28}$$

a building block for the inverse R-matrix is introduced by

$$I^{T[\overline{R}^{d_{12}d_{31}}_{d_{42}d_{34}}(\gamma)]}_{n,f}(\boldsymbol{\sigma};q) := (-1)^n \, I^{\overline{CS}}_{\boldsymbol{d},n,f}(\boldsymbol{\sigma};q) \, I^{\overline{R}}_{\boldsymbol{d},n,f}(\boldsymbol{\sigma};\boldsymbol{\gamma},q), \tag{3.29}$$

and labeled by $T[\overline{R}^{d_{12}d_{31}}_{d_{42}d_{34}}(\boldsymbol{\gamma})]$. By the specializations (3.18), the building block (3.29), in the massless limit as (3.19), yields the inverse R-matrix (3.3) with a normalization factor

in (3.10):

$$(-1)^{d_{23}} \, I_{n,f}^{T[\overline{R}_{d_{42}d_{34}}^{d_{12}d_{31}}(\gamma)]}(\boldsymbol{\sigma};q) \quad \rightarrow \quad q^{\frac{1}{4}n(n+2)} \left(R^{-1}\right)_{d_{42}+f \, d_{34}+f}^{d_{12}+f \, d_{31}+f}, \qquad (3.30)$$

where the prefactor $(-1)^{d_{23}}$ is introduced by the complexified FI parameters.

From above, the non-trivial degenerate inverse R-matrices

$$\left(R^{-1}\right)_{d_{42}d_{34}}^{d_{32}\ 0} = q^{\frac{1}{2}nd_{34}-\frac{1}{4}n^2} \frac{(q)_{n-d_{34}}}{(q)_{n-d_{32}}}, \qquad (3.31)$$

$$\left(R^{-1}\right)_{d_{32}\ 0}^{d_{12}d_{31}} = q^{-d_{12}d_{31}+\frac{1}{2}nd_{31}-\frac{1}{4}n^2} \frac{(q)_{d_{32}}(q)_n}{(q)_{n-d_{12}}(q)_{d_{12}}(q)_{d_{31}}}, \qquad (3.32)$$

$$\left(R^{-1}\right)_{0\ d_{12}}^{d_{12}\ 0} = \left(R^{-1}\right)_{d_{12}\ 0}^{0\ d_{12}} = q^{\frac{1}{2}nd_{12}-\frac{1}{4}n^2}, \qquad (3.33)$$

are also constructed by identifying some U(1) gauge symmetries, by identifying U(1)$_1$ with U(1)$_3$ for (3.31) and by identifying U(1)$_4$ with U(1)$_3$ for (3.32). The degenerate inverse R-matrix (3.33) is constructed in (4.3) just as a Chern-Simons factor.

3.2.3 Local minimum and maximum

The quantities $\mu_{d_{12}}$ and $\mu_{d_{12}}^{-1}$ for local minimum and maximum in (3.5) are constructed, by introducing gauge/flavor-R Chern-Simons couplings $k_1^{\text{g-R}} = \pm 2$, $k_2^{\text{g-R}} = \mp 2$, $k_c^{\text{f-R}} = \mp 1$ and $k_f^{\text{f-R}} = \pm 2$ from (2.20) as

$$I_{n,f}^{T[\mu_{d_{12}}]}(q) = q^{d_{12}+f-\frac{1}{2}n} = \mu_{d_{12}+f}, \qquad I_{n,f}^{T[\overline{\mu}_{d_{12}}]}(q) = q^{-d_{12}-f+\frac{1}{2}n} = \mu_{d_{12}+f}^{-1}, \qquad (3.34)$$

where d_1 and d_2 are the associated magnetic fluxes for a U(1)$_1 \times$ U(1)$_2$ gauge symmetry, and they are labeled by $T[\mu_{d_{12}}]$ and $T[\overline{\mu}_{d_{12}}]$.

3.3 K-theoretic vortex partitions in the knot-gauge theories

3.3.1 Summary

Because this section contains some technical details for the JK residue procedure and flux conditions, we first summarize what will be discussed.

From the building blocks in section 3.2, we can construct a U(1)^{N_v} knot-gauge theory $T[\mathcal{K}]$ labeled by a (1,1)-tangle diagram, with N_v crossings, of knot $\mathcal{K}$, and obtain the K-theoretic vortex partition[7]

$$I_{\text{vortex}}^{T[\mathcal{K}]}(\boldsymbol{\sigma};\boldsymbol{z},\boldsymbol{\gamma},q) = \sum_{\boldsymbol{d}} \left(\prod_{I=1}^{N_v} z_I^{d_I}\right) \prod_i I_{n,f}^{T_i}(\boldsymbol{\sigma};q), \qquad (3.35)$$

where $\boldsymbol{\sigma} = (\sigma_1,\ldots,\sigma_{N_v})$, $\boldsymbol{z} = (z_1,\ldots,z_{N_v})$ are the exponentiated FI parameters associated with the U(1)^{N_v} gauge symmetry, and $\boldsymbol{\gamma} = (\gamma_1,\ldots,\gamma_{2N_v})$ are mass parameters. Here i runs over all the building blocks labeled by T_i in (3.17), (3.29) and (3.34). By construction, if

---

[7]By the Reidemeister moves I, II and III for a tangle diagram of knot $\mathcal{K}$, infinitely many knot-gauge theories for $\mathcal{K}$ are constructed, and they are expected to be related to one another by some 3D dualities.

the conditions (3.2) and (3.4) for the magnetic fluxes $\boldsymbol{d}$ are satisfied, the K-theoretic vortex partition yields the normalized colored Jones polynomial $J_n^{\mathcal{K}}(q)$ of $\mathcal{K}$ under $\sigma_I \to \sigma_I^* = 1$, $\gamma_i \to \gamma_i^* = 1$, and $z_I \to z_I^* = +1$ or -1 depending on the sign factors in (3.20) and (3.30):

$$I_{\text{vortex}}^{T[\mathcal{K}]}(\boldsymbol{\sigma}^*; \boldsymbol{z}^*, \boldsymbol{\gamma}^*, q) = J_n^{\mathcal{K}}(q). \tag{3.36}$$

Therefore, for the relation (3.36), we need to choose the stability parameters so that the JK residue in (2.3) is taken at the locus $\sigma_I = \sigma_I^* = 1$ and the domain of the magnetic fluxes $\boldsymbol{d}$ is restricted by the conditions (3.2) and (3.4). In this paper, we consider a cone in (3.37) as a rough choice, where not only any choices of stability parameters inside the cone give the locus $\sigma_I = \sigma_I^* = 1$, but also, in general, some choices inside the cone may also give other loci (see Proposition 3.4 and (3.47) for an example). Therefore, for establishing the relation (3.36) we have to show that such other loci do not contribute to the twisted partition functions in the massless limit $\gamma_i \to \gamma_i^* = 1$. In section 3.3.3, we discuss conditions for the magnetic fluxes $\boldsymbol{d}$ which give non-zero contributions to the twisted partition functions in the massless limit. We first show Proposition 3.5 which implies the conditions (3.2) and (3.4) for the JK residue at the locus $\sigma_I = \sigma_I^* = 1$, and then discuss the contributions coming from the other loci. For our rough choice of the stability parameters, in Proposition 3.10 we find a class of knot diagrams such that the other loci do not contribute to the twisted partition functions in the massless limit and the relation (3.36) is established. We expect that, by carefully choosing the stability parameters, the relation (3.36) is, in general, established for any knot diagram.

Remark 3.2. In the context of knots-quivers correspondence [48, 49], the K-theoretic vortex partitions of abelian Chern-Simons-matter theories $T[Q_K]$ associated with quivers Q_K, which provide generating functions of S^n-colored HOMFLY-PT polynomials of knots K, and a class of 3D $\mathcal{N} = 2$ dualities associated with quivers, are discussed in [20, 50–53] (see also [54] for a different proposal of the relation between the K-theoretic vortex partitions and the HOMFLY-PT polynomials of torus knots). The 3D $\mathcal{N} = 2$ gauge theories $T[Q_K]$ seem to be quite different from the knot-gauge theories $T[\mathcal{K}]$ in this paper, and it would be interesting to clarify the relation between them.

3.3.2 JK residue procedure

Consider a $(1,1)$-tangle diagram with N_v crossings. As we constructed in the previous section, the matter content at the I-th crossing is composed of five chiral fields $\Phi_1^{(I)}$, $\Phi_2^{(I)}$, $\overline{\Phi}_3^{(I)}$, $\overline{\Phi}_4^{(I)}$ and $\Phi_5^{(I)}$ with the superpotential $W^{(I)} = \Phi_1^{(I)} \overline{\Phi}_4^{(I)} \Phi_5^{(I)} + \Phi_2^{(I)} \overline{\Phi}_3^{(I)} \Phi_5^{(I)}$, where we assume that $\Phi_1^{(I)}$, $\Phi_2^{(I)}$, $\overline{\Phi}_3^{(I)}$ and $\overline{\Phi}_4^{(I)}$ have generic masses $\gamma_1^{(I)}$, $\gamma_2^{(I)}$, $(\gamma_2^{(I)})^{-1}$ and $(\gamma_1^{(I)})^{-1}$, respectively, whereas $\Phi_5^{(I)}$ is massless. Let $Q_i^{(I)}$ be the U(1)^{N_v} gauge charge vectors of $\Phi_i^{(I)}$ and $\overline{\Phi}_i^{(I)}$, where $Q_5^{(I)}$, $I = 1, \ldots, N_v$, form a basis in $\mathbb{R}^{N_v}$, and have relations $-Q_5^{(I)} = Q_1^{(I)} + Q_4^{(I)} = Q_2^{(I)} + Q_3^{(I)}$. Here we take the gauge charge vectors to be zero for the incoming and outgoing chiral fields of the $(1,1)$-tangle diagram. For the JK residue [27, Theorem 2.6] (see also [28]), we choose the stability parameters (identified, in this paper, with the FI parameters) $\boldsymbol{\xi} = (\xi_1, \ldots, \xi_{N_v})$ inside Cone($\boldsymbol{Q}_5$) which is the cone spanned by

$\boldsymbol{Q}_5 = \{Q_5^{(I)}\}_{I=1,\ldots,N_v}$, i.e.,

$$\boldsymbol{\xi} = \sum_{I=1}^{N_v} c_I \, Q_5^{(I)} \in \mathrm{Cone}(\boldsymbol{Q}_5), \qquad c_I > 0. \tag{3.37}$$

We now need to consider the sets of the charge vectors for the poles, of the integrand in the twisted partition function, whose cones contain the vector (3.37) inside.

From $I_{\text{1-loop}}^{R}$ in (3.12) or $I_{\text{1-loop}}^{\overline{R}}$ in (3.24), once the residue at the (referred to as *massless*) pole "$\sigma_1 \sigma_4 = \sigma_2 \sigma_3$" relevant to $Q_5^{(I)}$ is taken, the (referred to as *massive*) poles relevant to $Q_i^{(I)}$, $i = 1, 2, 3, 4$, are moved away for generic masses. The charge vectors $\boldsymbol{Q}_5$ form a basis of $\mathbb{R}^{N_v}$, and the residues relevant to them boil down to the specializations $\sigma_1 = \sigma_2 = \ldots = \sigma_{N_v} = 1$ (i.e. (3.18)) of the complex scalars. Furthermore, as a corollary of Proposition 3.5 in section 3.3.3, when the residues at the poles relevant to $\boldsymbol{Q}_5$ are taken, the flux conditions (3.2) and (3.4) are also satisfied in the massless limit (3.19), where note that the poles relevant to $\boldsymbol{Q}_5$ imply the non-negativity of the magnetic fluxes for $\Phi_5^{(I)}$ at the crossings. As a result, if the other contributions in the JK residue are absent, the K-theoretic vortex partition function yields, in the massless limit, the normalized colored Jones polynomial as (3.36).

Therefore, the remaining problem is, for the choice of the stability parameters (3.37), whether other poles contribute to the twisted partition function in the massless limit.

Let $\Phi_i^{(I)}$ (resp. $\overline{\Phi}_i^{(I)}$) be an incoming (resp. outgoing) chiral field with $\mathrm{U}(1)_R$ charge $\mathsf{r} = 0$ (resp. $\mathsf{r} = 2$) assigned to the I-th crossing, where $i = 1$ or 2 (resp. 3 or 4). The chiral fields associated with an arc between the over I-th crossing and the over J-th crossing (or the under I-th crossing and the under J-th crossing) as

have opposite $\mathrm{U}(1)$ gauge charges, i.e. $Q_i^{(I)} = -Q_j^{(J)}$, where $i = 3$ or 4 and $j = 1$ or 2. On the other hand, the chiral fields associated with an arc between the over I-th crossing and the under J-th crossing (or the under I-th crossing and the over J-th crossing) as

have same $\mathrm{U}(1)$ gauge charges, i.e. $Q_i^{(I)} = Q_j^{(J)}$, where $i = 3$ or 4 and $j = 1$ or 2. Therefore, by the relations $-Q_5^{(I)} = Q_1^{(I)} + Q_4^{(I)} = Q_2^{(I)} + Q_3^{(I)}$, the charge vector $Q_5^{(I)}$ is expressed

as $Q_5^{(I)} = -Q_i^{(I)} + Q_j^{(J)} = Q_k^{(I)} - Q_\ell^{(J)}$ for (3.38) or $Q_5^{(I)} = -Q_i^{(I)} - Q_j^{(J)} = -Q_k^{(I)} - Q_\ell^{(J)}$ for (3.39), where $i, j = 1$ or 2 and $k, \ell = 3$ or 4.

For the over (resp. under) I-th crossing, let $P_+^{(I)}$ (resp. $P_-^{(I)}$), $\overline{P}_+^{(I)}$ (resp. $\overline{P}_-^{(I)}$), and $Q_+^{(I)}$ (resp. $Q_-^{(I)}$) be the charge vectors of $\Phi_1^{(I)}$ or $\Phi_2^{(I)}$, $\Phi_3^{(I)}$ or $\Phi_4^{(I)}$, and $\Phi_5^{(I)}$, respectively, where $P_\pm^{(I)} = Q_i^{(I)}$ for $i = 1$ or 2, $\overline{P}_\pm^{(I)} = Q_i^{(I)}$ for $i = 3$ or 4, and $Q_\pm^{(I)} = Q_5^{(I)}$. We now have $Q_\pm^{(I)} = -P_\pm^{(I)} + P_\pm^{(J)} = \overline{P}_\pm^{(I)} - \overline{P}_\pm^{(J)}$ for (3.38) and $Q_\pm^{(I)} = -P_\pm^{(I)} - P_\mp^{(J)} = -\overline{P}_\pm^{(I)} - \overline{P}_\mp^{(J)}$ for (3.39). The charge vectors $P_\pm^{(I)}$ are then expressed as

$$P_+^{(I)} = -\sum_{J \geq I} Q_+^{(J)} + \sum_{K \geq I} Q_-^{(K)}, \qquad P_-^{(I)} = -\sum_{J \geq I} Q_-^{(J)} + \sum_{K \geq I} Q_+^{(K)}, \qquad (3.40)$$

in terms of the basis $\boldsymbol{Q}_5 = \{Q_5^{(I)}\}_{I=1,\ldots,N_v}$, where the sum means that starting from the over (resp. under) I-th crossing, the over (resp. under) J-th crossings and the under (resp. over) K-th crossings pass through along the (1,1)-tangle diagram, and end at the last crossing with the bounded outgoing arc. Similarly, the charge vectors $\overline{P}_\pm^{(I)}$ are expressed as

$$\overline{P}_+^{(I)} = -\overline{\sum_{J \leq I}} Q_+^{(J)} + \overline{\sum_{K \leq I}} Q_-^{(K)}, \qquad \overline{P}_-^{(I)} = -\overline{\sum_{J \leq I}} Q_-^{(J)} + \overline{\sum_{K \leq I}} Q_+^{(K)}, \qquad (3.41)$$

where the sum means that starting from the over (resp. under) I-th crossing, the over (resp. under) J-th crossings and the under (resp. over) K-th crossings pass through, along the (1,1)-tangle diagram, backward, and end at the first crossing with the bounded incoming arc.

We now describe the (1,1)-tangle diagram by an ordered sequence of the charge vectors $Q_\pm^{(I)}$ by aligning them from the first crossing with the bounded incoming arc to the last crossing with the bounded outgoing arc along the tangle diagram. For convenience, we refer to the sequence as *original sequence*. For example, the $(1,1)$-tangle diagram of the trefoil knot $\boldsymbol{3_1}$ in figure 1 is described by a sequence

$$Q_+^{(1)}, \ Q_-^{(2)}, \ Q_+^{(3)}, \ Q_-^{(1)}, \ Q_+^{(2)}, \ Q_-^{(3)}. \qquad (3.42)$$

The following proposition is then proved.

Proposition 3.3. *For the stability parameters* (3.37), *if, in the original sequence, there exists a cyclic sequence* $\{Q_+^{(I_1)}, Q_-^{(I_2)}\}, \{Q_+^{(I_2)}, Q_-^{(I_3)}\}, \ldots, \{Q_+^{(I_{M-1})}, Q_-^{(I_M)}\}, \{Q_+^{(I_M)}, Q_-^{(I_1)}\}$ *consisted of adjacent pairs* $\{Q_+^{(I)}, Q_-^{(J)}\}$, *the residue at a massless pole relevant to one of the charge vectors* $Q_5^{(I_k)}$, $k = 1, \ldots, M$, *should be taken.*[8]

Proof. Consider the cyclic sequence in the assertion. By (3.40) and (3.41), all the charge vectors $Q_5^{(I)}$, $P_\pm^{(I)}$, $\overline{P}_\pm^{(I)}$ (i.e. $Q_i^{(I)}$) other than $Q_5^{(I_k)}$ satisfy $\sum_{k=1}^M Q_5^{(I_k)} = -1$ or 0 in terms of the basis $\boldsymbol{Q}_5$. This means that any cones consist of the charge vectors $Q_i^{(I)}$ without $Q_5^{(I_k)}$ do not contain the vector (3.37) inside, and the residues at a massless pole relevant to one of the charge vectors $Q_5^{(I_k)}$ should be taken. $\qquad \square$

---

[8]The order of the adjacent charge vectors $Q_+^{(I)}$ and $Q_-^{(J)}$ is not assumed.

Following Proposition 3.3 we should take the residue at the massless pole relevant to a charge vector $Q_5^{(I)}$ in each cyclic sequence, and then the massive pole around the I-th crossing is moved away. Therefore, for discussing cones which contain the vector (3.37) inside, it is enough to consider the subsequences (referred to as *reduced sequences*) extracted by removing the charge vectors $Q_5^{(I)}$ from the original sequence.[9] For example, for the original sequence (3.42) of $\mathbf{3_1}$ a reduced sequence

$$Q_+^{(1)}, \ Q_+^{(3)}, \ Q_-^{(1)}, \ Q_-^{(3)}, \tag{3.43}$$

is found by removing $Q_5^{(2)}$. When no reduced sequences are found, it is clear that, for the stability parameters (3.37), there are no cones, other than $\text{Cone}(\boldsymbol{Q}_5)$, which contain the vector (3.37) inside. If such cones, other than $\text{Cone}(\boldsymbol{Q}_5)$, exist, some reduced sequences should be found, and the following proposition is proved.

Proposition 3.4. *If there exist cones, other than* $\text{Cone}(\boldsymbol{Q}_5)$*, which contain the vector* (3.37) *inside, the spans of the cones should contain both some* $P_\pm^{(I)}$ *and some* $\overline{P}_\pm^{(J)}$*.*

Proof. To show the assertion, consider a cone consisted of $\boldsymbol{R} = \{R_I\}_{I=1,\dots,N_v} = \{P_\pm^{(I_\ell)}\}_{\ell=1,\dots,L} \ \cup \ \boldsymbol{Q}_5 \backslash \{Q_5^{(I_\ell)}\}_{\ell=1,\dots,L}$ or $\overline{\boldsymbol{R}} = \{\overline{R}_I\}_{I=1,\dots,N_v} = \{\overline{P}_\pm^{(I_\ell)}\}_{\ell=1,\dots,L} \ \cup \ \boldsymbol{Q}_5 \backslash \{Q_5^{(I_\ell)}\}_{\ell=1,\dots,L}$.

For the cone spanned by $\boldsymbol{R}$, starting from the first incoming arc, along the tangle in order, consider a part of the ordered sequence of charge vectors in $\{Q_5^{(I_\ell)}\}_{\ell=1,\dots,L}$,

$$\begin{aligned} &\dots, Q_+^{(J)}, \ Q_-^{(J_1)}, \ Q_-^{(J_2)}, \ \dots, \ Q_-^{(J_N)}, \ \dots, \\ \text{or} \quad &\dots, Q_-^{(J)}, \ Q_+^{(J_1)}, \ Q_+^{(J_2)}, \ \dots, \ Q_+^{(J_N)}, \ \dots, \end{aligned} \tag{3.44}$$

which is referred to as a *forward subsequence*. Similarly, for the cone spanned by $\overline{\boldsymbol{R}}$, consider

$$\begin{aligned} &\dots, Q_-^{(J_1)}, \ Q_-^{(J_2)}, \ \dots, \ Q_-^{(J_N)}, \ Q_+^{(J)}, \ \dots, \\ \text{or} \quad &\dots, Q_+^{(J_1)}, \ Q_+^{(J_2)}, \ \dots, \ Q_+^{(J_N)}, \ Q_-^{(J)}, \ \dots, \end{aligned} \tag{3.45}$$

which is referred to as a *backward subsequence*. The number of forward and backward subsequences is finite, and for all such subsequences as (3.44) and (3.45) we consider pairs $\{Q_+^{(J)}, Q_-^{(J_\ell)}\}$ or $\{Q_+^{(J_\ell)}, Q_-^{(J)}\}$, $\ell = 1, \dots, N$. The tangle passes through each crossing twice, and we then find at least one unbounded sequence of pairs as $\{Q_+^{(K_2)}, Q_-^{(K_1)}\}$, $\{Q_+^{(K_3)}, Q_-^{(K_2)}\}$, $\{Q_+^{(K_4)}, Q_-^{(K_3)}\}$, $\dots$ or $\{Q_+^{(K_1)}, Q_-^{(K_2)}\}$, $\{Q_+^{(K_2)}, Q_-^{(K_3)}\}$, $\{Q_+^{(K_3)}, Q_-^{(K_4)}\}$, $\dots$.[10] Furthermore, since this sequence is finite, as a subsequence of it, a cyclic sequence $\{Q_+^{(I_1)}, Q_-^{(I_2)}\}$, $\{Q_+^{(I_2)}, Q_-^{(I_3)}\}, \dots, \{Q_+^{(I_{M-1})}, Q_-^{(I_M)}\}$, $\{Q_+^{(I_M)}, Q_-^{(I_1)}\}$ should be obtained. Because any charge vectors $P_\pm^{(I)}$ in the set $\boldsymbol{R}$ (resp. $\overline{P}_\pm^{(I)}$ in the set $\overline{\boldsymbol{R}}$),

$$P_\pm^{(I)} \ (\text{resp. } \overline{P}_\pm^{(I)}) = \sum_{\ell=1}^M \left(\alpha_{\pm,\ell}^{(I)} Q_+^{(I_\ell)} + \beta_{\pm,\ell}^{(I)} Q_-^{(I_\ell)} \right) + \cdots = \sum_{\ell=1}^M \left(\alpha_{\pm,\ell}^{(I)} + \beta_{\pm,\ell}^{(I)} \right) Q_5^{(I_\ell)} + \cdots, \tag{3.46}$$

---

[9]By definition, the reduced sequences do not contain cyclic sequences in Proposition 3.3.

[10]As an example, if the ordered sequence starts as $Q_+^{(J_1)}, Q_+^{(J_2)}, Q_-^{(J_3)}, \dots$, the charge vectors except $Q_\pm^{(J_1)}$ can have pairs. In this case, by taking a first pair $\{Q_+^{(J_2)}, Q_-^{(J_3)}\}$, it is possible subsequently to find unbounded sequence of pairs as $\{Q_+^{(J_2)}, Q_-^{(J_3)}\}$, $\{Q_+^{(J_m)}, Q_-^{(J_2)}\}$, $\{Q_+^{(J_n)}, Q_-^{(J_m)}\}, \dots, m, n \neq 1$.

are expressed as (3.40) (resp. (3.41)) in terms of the basis $\boldsymbol{Q}_5$, we see that $\sum_{\ell=1}^{M} (\alpha_{\pm,\ell}^{(I)} + \beta_{\pm,\ell}^{(I)}) = -1$ if $P_{\pm}^{(I)}$ (resp. $\overline{P}_{\pm}^{(I)}$) is in between a pair in the cyclic sequence or $\sum_{\ell=1}^{M} (\alpha_{\pm,\ell}^{(I)} + \beta_{\pm,\ell}^{(I)}) = 0$ if otherwise, where $\cdots$ does not contain $Q_5^{(I_\ell)}$, $\ell = 1, \ldots, M$. Therefore, the cones spanned by $\boldsymbol{R}$ and $\overline{\boldsymbol{R}}$ do not contain the vector (3.37) inside, and our assertion follows. $\square$

The forward and backward subsequences in reduced sequences can be used to find cones other than $\text{Cone}(\boldsymbol{Q}_5)$. As an example, for the reduced sequence (3.43) of $\boldsymbol{3_1}$ we find a cyclic sequence $\{Q_+^{(3)}, Q_-^{(3)}\}$ from a forward subsequence and a cyclic sequence $\{Q_+^{(1)}, Q_-^{(1)}\}$ from a backward subsequence. Then, from the proof of Proposition 3.4, by considering $\overline{P}_-^{(1)}$ for $\{Q_+^{(3)}, Q_-^{(3)}\}$ and $P_+^{(3)}$ for $\{Q_+^{(1)}, Q_-^{(1)}\}$, we find a cone, which contains the vector (3.37) inside, consisted of

$$\overline{P}_-^{(1)} = Q_5^{(3)} - Q_5^{(2)}, \quad P_+^{(3)} = Q_5^{(1)} - Q_5^{(2)}, \quad Q_5^{(2)}, \tag{3.47}$$

for the original sequence (3.42) of $\boldsymbol{3_1}$. Therefore, we need to exclude this type of possibility

1) by showing that the contributions like (3.47) coming from cones other than $\text{Cone}(\boldsymbol{Q}_5)$ vanish, or;

2) if they do not vanish, by refining the choice of the stability parameters (3.37).

In the next subsection, we discuss flux conditions for the non-zero contributions to the twisted partition function, and then consider the first option. Actually, we will see that the cone (3.47) for $\boldsymbol{3_1}$ does not contribute in the massless limit (see Proposition 3.10).

3.3.3 Flux conditions

For flux conditions, the following proposition is proved.

Proposition 3.5. *When the magnetic fluxes for $\Phi_5^{(I)}$ at all the crossings are non-negative, the flux conditions (3.2) and (3.4) are satisfied in the massless limit.*

Proof. Assume that the magnetic fluxes for $\Phi_5^{(I)}$ at all the crossings are non-negative. When the magnetic flux at the I-th crossing is non-negative, i.e. the chiral field $\Phi_5^{(I)}$ gives a pole, at least, either $\Phi_1^{(I)}$ or $\Phi_4^{(I)}$ and either $\Phi_2^{(I)}$ or $\Phi_3^{(I)}$ give zeros as implied by the relations $-Q_5^{(I)} = Q_1^{(I)} + Q_4^{(I)} = Q_2^{(I)} + Q_3^{(I)}$ (the charges for $\text{U}(1)_c$ and $\text{U}(1)_{ext}$ also satisfy the same relations). Therefore, under the non-negative flux assumption, the number of zeros Z satisfies $Z \geq 2N_v$ and the number of poles P satisfies $P \leq 3N_v$, where $N_v = (Z + P)/5$ is the number of crossings. Because we take the residues at N_v poles, the contributions to the twisted partition function vanish, in the massless limit, if $Z > 2N_v$ ($P < 3N_v$), i.e. there exists a crossing such that both $\Phi_1^{(I)}$ and $\Phi_4^{(I)}$ or both $\Phi_2^{(I)}$ and $\Phi_3^{(I)}$ give zeros.

Let d_{in} and d_{out} be the magnetic fluxes for an incoming $\mathsf{r} = 0$ chiral field Φ and an outgoing $\mathsf{r} = 2$ chiral field $\overline{\Phi}$ for an (inverse) R-matrix assigned to a crossing, respectively. The non-negative flux assumption implies that the magnetic fluxes d_{in} and d_{out} for the

chiral fields along an under (resp. over) crossing arc satisfy $d_{\text{in}} \leq d_{\text{out}}$ (resp. $d_{\text{out}} \leq d_{\text{in}}$):

$$\text{under crossing}: \quad \begin{array}{c} \Phi \quad | \quad d_{in} \\ \hline \\ \overline{\Phi} \downarrow d_{out} \end{array} \qquad \text{over crossing}: \quad \begin{array}{c} \Phi \quad | \quad d_{in} \\ \hline \\ \overline{\Phi} \downarrow d_{out} \end{array}$$

$$d_{in} \leq d_{out} \qquad\qquad , \qquad\qquad d_{out} \leq d_{in} \qquad\qquad . \qquad (3.48)$$

For the under (I-th) crossing, if $\Phi^{(I)}$ gives a zero and $\overline{\Phi}^{(I)}$ gives a pole, i.e. $d_{\text{in}}^{(I)} \leq d_{\text{out}}^{(I)} < 0$, then $d_{\text{in}}^{(I+1)}(= d_{\text{out}}^{(I)}) < 0$ at the next (($I+1$)-th) crossing which results in $d_{\text{out}}^{(I+1)} < 0$ for the non-zero contributions to the twisted partition function in the massless limit. Since the last outgoing magnetic flux at the last crossing is given by a background magnetic flux $f \in \{0, 1, \ldots, n\}$ for the global symmetry $\text{U}(1)_{ext}$ (e.g. see figure 1), the gluing procedure excludes the case $d_{\text{in}}^{(I)} \leq d_{\text{out}}^{(I)} < 0$ for the under crossing arc. Similarly, the case $n < d_{\text{out}} \leq d_{\text{in}}$ for an over crossing arc is also excluded. As a result, the magnetic fluxes are constrained by the conditions

$$0 \leq d_{\text{in}} \leq d_{\text{out}} \quad \text{(under crossing)}, \qquad d_{\text{out}} \leq d_{\text{in}} \leq n \quad \text{(over crossing)}, \qquad (3.49)$$

which mean all $\Phi^{(I)}$ give poles and all $\overline{\Phi}^{(I)}$ give zeros.

Starting from a crossing with the magnetic fluxes d_{in} and d_{out} with the conditions (3.49), in the sequel of gluing procedure along the tangle in order, if the outgoing under (resp. over) crossing arc is glued with an over (resp. under) crossing incoming arc first at the K-th crossing we find $0 \leq d_{\text{in}} \leq d_{\text{out}} \leq \ldots \leq d_K \leq n$ (resp. $0 \leq d_K \leq \ldots \leq d_{\text{out}} \leq d_{\text{in}} \leq n$), where d_K is the magnetic flux for the incoming chiral field assigned to the K-th crossing. Even if the outgoing under (resp. over) crossing arcs are only glued with under (resp. over) crossing incoming arcs, because the gluing procedure ends up with the background magnetic flux $f \in \{0, 1, \ldots, n\}$, we find $0 \leq d_{\text{in}}, d_{\text{out}} \leq n$ anyway. This gives the desired conditions in (3.2) and (3.4). $\qquad \square$

Proposition 3.4 and 3.5 imply the following corollary.

Corollary 3.6. *For the stability parameters (3.37), the cones other than $\text{Cone}(\boldsymbol{Q}_5)$ do not contribute to the twisted partition function in the massless limit when the magnetic fluxes for $\Phi_5^{(I)}$ at all the crossings are non-negative.*

Next, we consider the cases with negative fluxes for some $\Phi_5^{(I)}$. Let E_v be the number of negative fluxes for $\Phi_5^{(I)}$, and then the number of non-negative fluxes for $\Phi_5^{(I)}$ is $N_v - E_v$, where N_v is the number of crossings. As the proof of Proposition 3.5, we see that the number of zeros Z satisfies $Z \geq 2(N_v - E_v) + E_v = 2N_v - E_v$. Therefore, for the condition $Z > 2N_v$ of the vanishing contributions to the twisted partition function in the massless limit, it needs, at least, $E_v + 1$ extra zeros in addition to the minimal number of zeros. From a reduced sequence, let us extract the subsequence composed of all of the E_v charge vectors with negative fluxes for $\Phi_5^{(I)}$, and, in what follows, we refer to it as *negative sequence*:

$$\text{original sequence} \supset \text{reduced sequence} \supset \text{negative sequence}. \qquad (3.50)$$

For negative sequences, the following proposition is proved.

Proposition 3.7. *For a negative sequence, in addition to the minimal number of zeros $2N_v - E_v$, there is at least one extra zero*

(1) *after the last charge vector $Q_+^{(I)}$ or $Q_-^{(I)}$ in the negative sequence;*

(2) *between adjacent charge vectors $Q_+^{(I)}$ and $Q_+^{(J)}$ or $Q_-^{(I)}$ and $Q_-^{(J)}$ in the negative sequence;*

(3) *for each cyclic sequence $\{Q_+^{(I_1)}, Q_-^{(I_2)}\}$, $\{Q_+^{(I_2)}, Q_-^{(I_3)}\}$, ... , $\{Q_+^{(I_{M-1})}, Q_-^{(I_M)}\}$, $\{Q_+^{(I_M)}, Q_-^{(I_1)}\}$ consisted of adjacent pairs $\{Q_+^{(I)}, Q_-^{(J)}\}$ in the negative sequence, when the stability parameters (3.37) are assumed.*

Proof. (1) Consider the last charge vector $Q_+^{(I)}$ (resp. $Q_-^{(I)}$) in a negative sequence. If the $\mathsf{r} = 2$ chiral field with the charge vector $\overline{P}_+^{(I)}$ (resp. $\overline{P}_-^{(I)}$) gives a pole, the relevant flux d_{out} satisfies $d_{\text{out}} > n$ (resp. $d_{\text{out}} < 0$). Since the last outgoing $\mathsf{r} = 2$ chiral field has a background magnetic flux $f \in \{0, 1, \ldots, n\}$, by (3.48), there should be a charge vector $Q_+^{(K)}$ (resp. $Q_-^{(K)}$) with non-negative flux in the original sequence after $Q_+^{(I)}$ (resp. $Q_-^{(I)}$), and both $\mathsf{r} = 0$ chiral field with the charge vector $P_+^{(K)}$ (resp. $P_-^{(K)}$) and $\mathsf{r} = 2$ chiral field with the charge vector $\overline{P}_+^{(K)}$ (resp. $\overline{P}_-^{(K)}$) give zeros. This shows the assertion (1).

(2) Assume that there are adjacent charge vectors $Q_+^{(I)}$ and $Q_+^{(J)}$ in a negative sequence. If both $\mathsf{r} = 2$ chiral field with the charge vector $\overline{P}_+^{(I)}$ and $\mathsf{r} = 0$ chiral field with the charge vector $P_+^{(J)}$ give pole, the former relevant flux d_{out} satisfies $d_{\text{out}} > n$ whereas the latter relevant flux d_{in} satisfies $d_{\text{in}} < n$. Therefore, similarly to the proof of the assertion (1), there should be at least one extra zero between $Q_+^{(I)}$ and $Q_+^{(J)}$. Similarly, the assertion for adjacent charge vectors $Q_-^{(I)}$ and $Q_-^{(J)}$ is proved.

(3) Assume that there is the cyclic sequence in the assertion. To have a cone which contains the vector (3.37) inside, by considering $\sum_{k=1}^{M} Q_5^{(I_k)}$ (cf. the proof of Proposition 3.3), we see that there should be a charge vector $Q_+^{(K)}$ (resp. $Q_-^{(K)}$) with non-negative flux in the original sequence between

(i) a pair of adjacent charge vectors in the negative sequence ordered as $Q_+^{(I_k)}$, $Q_-^{(I_{k+1})}$, where the $\mathsf{r} = 0$ (resp. $\mathsf{r} = 2$) chiral field with the charge vector $P_+^{(K)}$ (resp. $\overline{P}_-^{(K)}$) gives a pole, or;

(ii) a pair of adjacent charge vectors in the negative sequence ordered as $Q_-^{(I_{k+1})}$, $Q_+^{(I_k)}$, where the $\mathsf{r} = 2$ (resp. $\mathsf{r} = 0$) chiral field with the charge vector $\overline{P}_+^{(K)}$ (resp. $P_-^{(K)}$) gives a pole.

In the case (i), if the $\mathsf{r} = 2$ chiral field with the charge vector $\overline{P}_+^{(I_k)}$ gives a pole, the relevant flux d_{out} satisfies $d_{\text{out}} > n$ whereas the flux d_{in} relevant to $P_+^{(K)}$ (resp. $P_-^{(K)}$) satisfies $d_{\text{in}} < n$ (resp. $d_{\text{in}} < 0$). Therefore, at least one extra zero between $Q_+^{(I_k)}$ and $Q_+^{(K)}$ (resp. $Q_-^{(K)}$) should be found. Similarly, in the case (ii), at least one extra zero between $Q_-^{(I_{k+1})}$ and $Q_+^{(K)}$ (resp. $Q_-^{(K)}$) should be found. $\square$
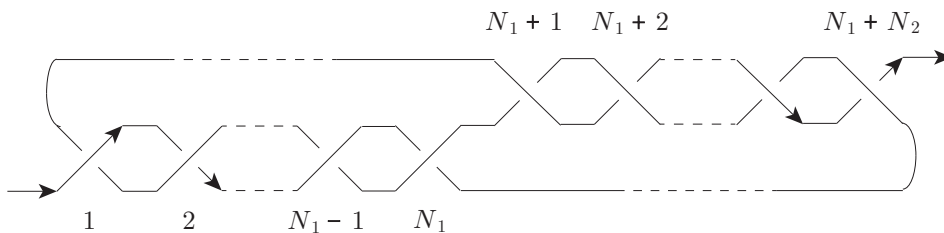
Figure 4. A $(1,1)$-tangle diagram of a 2-bridge knot (rational knot) with (N_1, N_2) twists, where $N_1 \geq N_2 \geq 0$.

When $E_v = 1$, the ordered negative sequences are $(Q_\pm^{(1)}, Q_\mp^{(1)})$, and Proposition 3.7 implies, at least, two extra zeros in addition to $2N_v - 1$ zeros. When $E_v = 2$, the ordered negative sequences are

$$(Q_\pm^{(1)}, Q_\pm^{(2)}, Q_\mp^{(1)}, Q_\mp^{(2)}), \ (Q_\pm^{(1)}, Q_\mp^{(1)}, Q_\pm^{(2)}, Q_\mp^{(2)}),$$
$$(Q_\pm^{(1)}, Q_\mp^{(2)}, Q_\pm^{(2)}, Q_\mp^{(1)}), \ (Q_\pm^{(1)}, Q_\mp^{(2)}, Q_\mp^{(1)}, Q_\pm^{(2)}), \tag{3.51}$$

which imply, at least, three extra zeros in addition to $2N_v - 2$ zeros, and

$$(Q_\pm^{(1)}, Q_\pm^{(2)}, Q_\mp^{(2)}, Q_\mp^{(1)}), \ (Q_\pm^{(1)}, Q_\mp^{(1)}, Q_\mp^{(2)}, Q_\pm^{(2)}), \tag{3.52}$$

which imply, at least, four extra zeros in addition to $2N_v - 2$ zeros. Therefore, we have the following corollary.

Corollary 3.8. *For the stability parameters* (3.37), *the cones other than* $\mathrm{Cone}(\boldsymbol{Q}_5)$ *do not contribute to the twisted partition function in the massless limit when the number of negative fluxes for* $\Phi_5^{(I)}$ *is up to* $E_v = 2$.

From the negative sequences (3.51) and (3.52) with $E_v = 2$, we make negative sequences with $E_v = E_1 + E_2$ by replacements

$$Q_\pm^{(1)} \ \to \ Q_\pm^{(1, J_1^\pm)}, \ Q_\pm^{(1, J_2^\pm)}, \ \ldots, \ Q_\pm^{(1, J_{E_1}^\pm)}, \quad Q_\pm^{(2)} \ \to \ Q_\pm^{(2, K_1^\pm)}, \ Q_\pm^{(2, K_2^\pm)}, \ \ldots, \ Q_\pm^{(2, K_{E_2}^\pm)},$$
$$\tag{3.53}$$

where $\{J_1^\pm, J_2^\pm, \ldots, J_{E_1}^\pm\} = \{1, 2, \ldots, E_1\}$ and $\{K_1^\pm, K_2^\pm, \ldots, K_{E_2}^\pm\} = \{1, 2, \ldots, E_2\}$. We see that Proposition 3.7 also implies the following corollary.

Corollary 3.9. *For the stability parameters* (3.37), *the cones other than* $\mathrm{Cone}(\boldsymbol{Q}_5)$ *do not contribute to the twisted partition function in the massless limit when the negative sequences take the above forms by the replacements* (3.53).

Let us consider a $(1,1)$-tangle diagram of a 2-bridge knot (rational knot) with (N_1, N_2) twists $(N_1 \geq N_2 \geq 0)$ in figure 4 whose original sequence is one of the following forms:

$$(Q_+^{(1)}, \ Q_-^{(2)}, \ \ldots, \ Q_-^{(N_1)}; \ Q_+^{(N_1+N_2)}, \ Q_-^{(N_1+N_2-1)}, \ \ldots, \ Q_-^{(N_1+1)};$$
$$Q_+^{(N_1)}, \ Q_-^{(N_1-1)}, \ \ldots, \ Q_-^{(1)}; \ Q_+^{(N_1+1)}, \ Q_-^{(N_1+2)}, \ \ldots, \ Q_-^{(N_1+N_2)}),$$

$$\begin{aligned}
(Q_+^{(1)}, \ Q_-^{(2)}, \ \ldots, \ Q_+^{(N_1)}; \ Q_-^{(N_1+1)}, \ Q_+^{(N_1+2)}, \ \ldots, \ Q_+^{(N_1+N_2)}; \\
Q_-^{(N_1)}, \ Q_+^{(N_1-1)}, \ \ldots, \ Q_-^{(1)}; \ Q_+^{(N_1+1)}, \ Q_-^{(N_1+2)}, \ \ldots, \ Q_-^{(N_1+N_2)}), \\
(Q_+^{(1)}, \ Q_-^{(2)}, \ \ldots, \ Q_-^{(N_1)}; \ Q_+^{(N_1+N_2)}, \ Q_-^{(N_1+N_2-1)}, \ \ldots, \ Q_+^{(N_1+1)}; \\
Q_-^{(1)}, \ Q_+^{(2)}, \ \ldots, \ Q_+^{(N_1)}; \ Q_-^{(N_1+1)}, \ Q_+^{(N_1+2)}, \ \ldots, \ Q_-^{(N_1+N_2)}),
\end{aligned} \qquad (3.54)$$

where the first, second, and third cases correspond to the cases with $(N_1, N_2) = (\text{even}, \text{even})$, $(N_1, N_2) = (\text{odd}, \text{even})$, and $(N_1, N_2) = (\text{even}, \text{odd})$, respectively. In particular, they include twist knots e.g. as

$$\begin{aligned}
(N_1, N_2) = (2, 1): \ \mathbf{3_1}, \quad (N_1, N_2) = (2, 2): \ \mathbf{4_1}, \quad (N_1, N_2) = (3, 2): \ \mathbf{5_2}, \\
(N_1, N_2) = (4, 2): \ \mathbf{6_1}, \quad (N_1, N_2) = (5, 2): \ \mathbf{7_2}, \quad (N_1, N_2) = (6, 2): \ \mathbf{8_1}, \ etc.,
\end{aligned} \qquad (3.55)$$

in the Rolfsen table. For the original sequences in (3.54), because the reduced sequences take the forms constructed by the replacements (3.53), any negative sequences for them also take the forms constructed by the replacements (3.53). Then, as a result of Corollary 3.9, we find the following proposition.

Proposition 3.10. *For the stability parameters* (3.37), *the factorization of the twisted partition function on* $\mathbb{S}^2 \times_q \mathbb{S}^1$ *for the* $(1, 1)$-*tangle diagram of the 2-bridge knot in figure 4 gives the K-theoretic vortex partition function which agrees, in the massless limit and the exponentiated FI parameters* $z_I \to +1$ *or* -1 *limit depending on the prefactors in* (3.20) *and* (3.30), *with the normalized colored Jones polynomial of the 2-bridge knot.*

In the next subsection, we describe an explicit computation for the trefoil knot $\mathbf{3_1}$ as the simplest example of Proposition 3.10.

Remark 3.11. When we consider more general tangle diagrams, for a choice of the stability parameters in (3.37), some cones other than $\text{Cone}(\boldsymbol{Q}_5)$ may contribute to the twisted partition function in the massless limit. For such cases, the second option described at the end of section 3.3.2 (i.e. more appropriate choices of the stability parameters) should be considered. We leave them for future research.
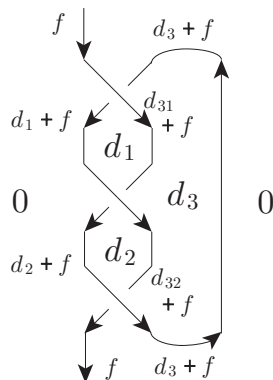
3.4 Examples

3.4.1 Trefoil knot $\mathbf{3_1}$

As the simplest non-trivial example, consider a $(1, 1)$-tangle diagram of the trefoil knot $\mathbf{3_1}$ in figure 5 (figure 1). The associated $\text{U}(1)^3$ knot-gauge theory $T[\mathbf{3_1}]$ has the chiral fields in table 3 and Chern-Simons couplings

$$\begin{aligned}
k_{11} = k_{22} = k_1^{\text{g-R}} = k_2^{\text{g-R}} = 1, \qquad k_{33} = -\frac{3}{2}, \qquad k_{12} = k_{21} = -\frac{1}{2}, \qquad k_3^{\text{g-R}} = \frac{1}{2}, \\
k_{3c}^{\text{g-f}} = \frac{3}{2}, \quad k_{3f}^{\text{g-f}} = -3, \quad k_c^{\text{f-R}} = 2, \qquad k_{cf}^{\text{f-f}} = k_{fc}^{\text{f-f}} = 3, \qquad k_{ff}^{\text{f-f}} = -6, \quad k_f^{\text{f-R}} = 2,
\end{aligned} \qquad (3.56)$$

and is considered to be a coupled system of the theories labeled by

$$\begin{aligned}
T_1 = T[\overline{R}_{d_1 d_{31}}^{\ 0 \ d_3}(\gamma_{1,1}, \gamma_{1,2})], \quad T_2 = T[\overline{R}_{d_2 d_{32}}^{d_1 d_{31}}(\gamma_{2,1}, \gamma_{2,2})], \\
T_3 = T[\overline{R}_{0 \ d_3}^{d_2 d_{32}}(\gamma_{3,1}, \gamma_{3,2})], \quad T_4 = T[\mu_{d_3}],
\end{aligned} \qquad (3.57)$$

Figure 5. $(1,1)$-tangle diagram of the trefoil knot $\mathbf{3_1}$, where $f \in \{0, 1, \ldots, n\}$ is fixed.

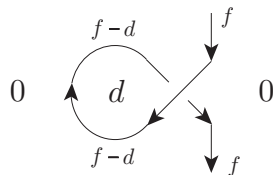| Field	U(1)$_1$	U(1)$_2$	U(1)$_3$	U(1)$_c$	U(1)$_{ext}$	mass	U(1)$_R$
$\Phi_1^{(1)}$	0	0	0	1	-1	$\gamma_{1,1}$	0
$\Phi_2^{(1)}$	0	0	1	0	1	$\gamma_{1,2}$	0
$\overline{\Phi}_3^{(1)}$	-1	0	0	0	-1	$\gamma_{1,2}^{-1}$	2
$\overline{\Phi}_4^{(1)}$	-1	0	1	-1	1	$\gamma_{1,1}^{-1}$	2
$\Phi_5^{(1)}$	1	0	-1	0	0	1	0
$\Phi_1^{(2)}$	-1	0	0	1	-1	$\gamma_{2,1}$	0
$\Phi_2^{(2)}$	-1	0	1	0	1	$\gamma_{2,2}$	0
$\overline{\Phi}_3^{(2)}$	0	-1	0	0	-1	$\gamma_{2,2}^{-1}$	2
$\overline{\Phi}_4^{(2)}$	0	-1	1	-1	1	$\gamma_{2,1}^{-1}$	2
$\Phi_5^{(2)}$	1	1	-1	0	0	1	0
$\Phi_1^{(3)}$	0	-1	0	1	-1	$\gamma_{3,1}$	0
$\Phi_2^{(3)}$	0	-1	1	0	1	$\gamma_{3,2}$	0
$\overline{\Phi}_3^{(3)}$	0	0	0	0	-1	$\gamma_{3,2}^{-1}$	2
$\overline{\Phi}_4^{(3)}$	0	0	1	-1	1	$\gamma_{3,1}^{-1}$	2
$\Phi_5^{(3)}$	0	1	-1	0	0	1	0

Table 3. Matter content for the $(1,1)$-tangle diagram of the trefoil knot $\mathbf{3_1}$ in figure 5 corresponding to the inverse R-matrices for (3.57), where U(1)$_{ext}$ and U(1)$_c$ are global symmetries.

where $d_{ij} = d_i - d_j$, and $\boldsymbol{\gamma} = (\gamma_{1,1}, \gamma_{1,2}, \gamma_{2,1}, \gamma_{2,2}, \gamma_{3,1}, \gamma_{3,2})$ are mass parameters. The K-theoretic vortex partition function is given by

$$I_{\text{vortex}}^{T[\mathbf{3_1}]}(\boldsymbol{\sigma}; \boldsymbol{z}, \boldsymbol{\gamma}, q) = \sum_{d_1, d_2, d_3} z_1^{d_1} z_2^{d_2} z_3^{d_3} \prod_{i=1}^{4} I_{n,f}^{T_i}(\boldsymbol{\sigma}; q), \tag{3.58}$$

where $\boldsymbol{\sigma} = (\sigma_1, \sigma_2, \sigma_3)$, and $\boldsymbol{z} = (z_1, z_2, z_3)$ are the exponentiated FI parameters associated with the U(1)$_1 \times$ U(1)$_2 \times$ U(1)$_3$ gauge symmetry. For the FI parameters $\xi_I = -\text{Re}(\log z_I)$, $I = 1, 2, 3$, inside Cone(Q_1, Q_2, Q_3), only the JK residue at $\boldsymbol{\sigma} = \boldsymbol{\sigma}^* = (1, 1, 1)$ finally contributes, where $Q_1 = (1, 0, -1)$, $Q_2 = (1, 1, -1)$, and $Q_3 = (0, 1, -1)$ are, respectively, the charge vectors of $\Phi_5^{(1)}$, $\Phi_5^{(2)}$, and $\Phi_5^{(3)}$ for the U(1)$_1 \times$ U(1)$_2 \times$ U(1)$_3$ gauge symmetry.

Figure 6. $(1,1)$-tangle diagram of the unknot.

Field	U(1)	U(1)$_c$	U(1)$_{ext}$	mass	U(1)$_R$
Φ_1	-1	0	1	γ_1	0
Φ_2	0	1	-1	γ_2	0
$\overline{\Phi}_3$	-1	-1	1	γ_2^{-1}	2
$\overline{\Phi}_4$	0	0	-1	γ_1^{-1}	2
Φ_5	1	0	0	1	0

Table 4. Matter content for the tangle diagram in figure 6 corresponding to the R-matrix $R_{f-d\,f}^{f-d\,f}$, where U(1)$_{ext}$ and U(1)$_c$ are global symmetries.

Then, under $\boldsymbol{z} \to \boldsymbol{z}^* = (1,1,-1)$ following (3.30) and $\boldsymbol{\gamma} \to \boldsymbol{\gamma}^*$ with $\gamma_{k,\ell}^* = 1$, the K-theoretic vortex partition function (3.58) yields the normalized colored Jones polynomial of $\mathbf{3_1}$:

$$
\begin{aligned}
I_{\text{vortex}}^{T[\mathbf{3_1}]}&(\sigma^*; \boldsymbol{z}^*, \boldsymbol{\gamma}^*, q) \\
&= q^{\frac{3}{4}n(n+2)} \sum_{\substack{0 \le d_{13}, d_{23} \le f \\ -d_{13}-d_{23} \le d_3 \le n-f}} \left(R^{-1}\right)_{d_1+f\ d_{31}+f}^{f\qquad d_3+f} \\
&\qquad\qquad\qquad \times \left(R^{-1}\right)_{d_2+f\ d_{32}+f}^{d_1+f\ d_{31}+f} \left(R^{-1}\right)_{f\qquad d_3+f}^{d_2+f\ d_{32}+f} \mu_{d_3+f} \\
&= J_n^{\mathbf{3_1}}(q) \\
&= \sum_{\substack{0 \le d_{13}, d_{23} \le f \\ -d_{13}-d_{23} \le d_3 \le n-f}} q^{d_{13}^2+d_{23}^2+(d_{13}+d_{23}-3f+1)d_3+(d_3-d_{13}-d_{23}+3f+1)n-3f^2+f} \\
&\qquad \times \frac{(q)_{d_{13}+d_3+f}\,(q)_{n-f+d_{13}}\,(q)_{d_{23}+d_3+f}\,(q)_{n-f+d_{23}}\,(q)_f\,(q)_{n-f-d_3}}{(q)_{f-d_{13}}\,(q)_{d_{13}}\,(q)_{n-f-d_{13}-d_3}\,(q)_{f-d_{23}}\,(q)_{d_{23}}\,(q)_{n-f-d_{23}-d_3}\,(q)_{d_{13}+d_{23}+d_3}\,(q)_{d_3+f}\,(q)_{n-f}},
\end{aligned}
$$
(3.59)

where note that $(q)_d^{-1} = 0$ for $d \in \mathbb{Z}_{<0}$, and we can check that the result does not depend on the constant $f \in \{0, 1, \ldots, n\}$.

3.4.2 Unknot and Reidemeister move I

Consider a $(1,1)$-tangle diagram of the unknot in figure 6. Then, the U(1) knot-gauge theory $T[\mathbf{0}]$ with chiral fields in table 4 and Chern-Simons couplings

$$
k = \frac{1}{2}, \quad k_c^{\text{g-f}} = \frac{1}{2}, \quad k_f^{\text{g-f}} = -1, \quad k^{\text{g-R}} = \frac{3}{2}, \quad k_{cf}^{\text{f-f}} = k_{fc}^{\text{f-f}} = -1, \quad k_{ff}^{\text{f-f}} = 2, \quad k_f^{\text{f-R}} = -2,
$$
(3.60)

which is considered to be a coupled system of two theories labeled by

$$T_1 = T[R_{-d\,0}^{-d\,0}(\boldsymbol{\gamma})], \quad T_2 = T[\overline{\mu}_{-d}], \tag{3.61}$$

is associated, where $\boldsymbol{\gamma} = (\gamma_1, \gamma_2)$ are mass parameters. The K-theoretic vortex partition function is given by

$$I_{\text{vortex}}^{T[\mathbf{0}]}(\sigma; z, \boldsymbol{\gamma}, q) = \sum_d z^d \, I_{n,f}^{T_1}(\sigma; q) \, I_{n,f}^{T_2}(q). \tag{3.62}$$

Here the exponentiated FI parameter z associated with the U(1) gauge symmetry is taken as $-\mathrm{Re}(\log z) > 0$, and then the residue at $\sigma = \sigma^* = 1$ relevant to Φ_5 is taken. As a result, the K-theoretic vortex partition function yields, by $z \to z^* = 1$ following (3.20) and $\boldsymbol{\gamma} \to \boldsymbol{\gamma}^* = (1, 1)$, the normalized colored Jones polynomial of unknot:

$$
\begin{aligned}
I_{\text{vortex}}^{T[\mathbf{0}]}(\sigma^*; z^*, \boldsymbol{\gamma}^*, q) &= q^{-\frac{1}{4}n(n+2)} \sum_{0 \leq d \leq f} R_{f-d\,f}^{f-d\,f} \mu_{f-d}^{-1} = J_n^{\mathbf{0}}(q) \\
&= \sum_{0 \leq d \leq f} (-1)^d \, q^{\frac{1}{2}d(d+1)-fd-f(n-f+1)} \frac{(q)_{n-f+d}\,(q)_f}{(q)_{f-d}\,(q)_{n-f}\,(q)_d} \\
&= 1.
\end{aligned}
\tag{3.63}
$$

Here the last equality is obvious for $f = 0$ and, in general, follows from the fact that it equals to the one by $n \to n-1$ and $f \to f-1$, i.e.,

$$\sum_{0 \leq d \leq f-1} (-1)^d \, q^{\frac{1}{2}d(d+1)-(f-1)d-(f-1)(n-f+1)} \frac{(q)_{n-f+d}\,(q)_{f-1}}{(q)_{f-d-1}\,(q)_{n-f}\,(q)_d},$$

which can be shown by the following q-Pascal relation

$$\frac{(q)_{m+n}}{(q)_m\,(q)_n} = \frac{(q)_{m+n-1}}{(q)_{m-1}\,(q)_n} + q^m \frac{(q)_{m+n-1}}{(q)_m\,(q)_{n-1}}, \tag{3.64}$$

with $m = f - d$ and $n = d$. The result (3.63) is understood by the Reidemeister move I.

4 Reduced knot-gauge theory

In this section, we consider $(1, 1)$-tangle diagrams with the external incoming (outgoing) constant $f = 0$ such that the first incoming arc is over crossing and the last outgoing arc is under crossing. On this basis, the (inverse) R-matrices assigned to the first and last crossings are extremely degenerated, and the corresponding gauge theories are simplified. As the examples, we describe the trefoil knot $\mathbf{3_1}$, the figure-eight knot $\mathbf{4_1}$ and the 3-twist knot $\mathbf{5_2}$.

4.1 Setup

We assume the following setup for a $(1, 1)$-tangle diagram of a knot $\mathcal{K}$ [42, 46] (see figure 7, 8 and 9 for examples):

1. The tangle starts from an over crossing arc and ends with an under crossing arc.

2. Trivial external incoming (outgoing) constant $f = 0$ is assigned at the end points of the tangle diagram.

By the last conditions in (3.2) and (3.4), this setup implies that the R-matrices assigned to the first and last crossings have degenerated forms (3.23) or (3.33). Instead of introducing chiral fields in section 3.2, we construct them with normalization factors in (3.10) just as Chern-Simons factors in (2.20), with non-zero Chern-Simons couplings $k_{1c}^{\text{g-f}} = \mp 1/2$, $k_{2c}^{\text{g-f}} = \pm 1/2$ and $k_c^{\text{f-R}} = \mp 1$:

$$I_{d_{12},n}^{\text{CS}_+}(\boldsymbol{\sigma};q) = \left(\frac{\sigma_1}{\sigma_2}\right)^{-\frac{1}{2}n} q^{-\frac{1}{2}nd_{12}-\frac{1}{2}n}, \qquad I_{d_{12},n}^{\text{CS}_-}(\boldsymbol{\sigma};q) = \left(\frac{\sigma_1}{\sigma_2}\right)^{\frac{1}{2}n} q^{\frac{1}{2}nd_{12}+\frac{1}{2}n}, \qquad (4.1)$$

as

$$I_n^{T[R^{d_{12}\ 0}_{\ \ 0\ d_{12}}]}(q) = I_n^{T[R^{\ 0\ d_{12}}_{d_{12}\ 0}]}(q) = I_{d_{12},n}^{\text{CS}_+}(\boldsymbol{\sigma};q)$$
$$= q^{-\frac{1}{4}n(n+2)} R^{d_{12}\ 0}_{\ \ 0\ d_{12}} = q^{-\frac{1}{4}n(n+2)} R^{\ 0\ d_{12}}_{d_{12}\ 0}, \qquad (4.2)$$

$$I_n^{T[\overline{R}^{d_{12}\ 0}_{\ \ 0\ d_{12}}]}(q) = I_n^{T[\overline{R}^{\ 0\ d_{12}}_{d_{12}\ 0}]}(q) = I_{d_{12},n}^{\text{CS}_-}(\boldsymbol{\sigma};q)$$
$$= q^{\frac{1}{4}n(n+2)} \left(R^{-1}\right)^{d_{12}\ 0}_{\ \ 0\ d_{12}} = q^{\frac{1}{4}n(n+2)} \left(R^{-1}\right)^{\ 0\ d_{12}}_{d_{12}\ 0}, \qquad (4.3)$$

where $\boldsymbol{\sigma} = (\sigma_1, \sigma_2)$ are the complex scalars for a gauge symmetry $\text{U}(1)_1 \times \text{U}(1)_2$. Here, as in footnote 6, the $\text{U}(1)_1$-$\text{U}(1)_c$ and $\text{U}(1)_2$-$\text{U}(1)_c$ parity anomalies are shown to be absent for each loop.

In the following, we will represent the arcs with the trivial constant 0, like the first and last ones, by dashed lines. If the second crossing after the first over crossing is also over crossing, the second arc is also represented by the dashed line, and the same applies to the subsequent and last crossings. Let n_v be the number of loops in the tangle diagram after removing the dashed lines. Then a $\text{U}(1)^{n_v}$ gauge theory $T^{\text{red}}[\mathcal{K}]$ is constructed similarly as section 3, and Proposition 3.10 is also established because the charge vectors like $Q_+^{(1)}$ and $Q_-^{(N_1+N_2)}$ are just removed from the original sequences in (3.54). The gauge theory $T^{\text{red}}[\mathcal{K}]$ is simpler than the knot-gauge theories $T[\mathcal{K}]$ in section 3, and we refer to it as the reduced knot-gauge theory.

4.2 Examples

4.2.1 Trefoil knot 3_1

Consider the reduced $\text{U}(1)$ knot-gauge theory $T^{\text{red}}[\mathbf{3_1}]$ for a $(1,1)$-tangle diagram of the trefoil knot $\mathbf{3_1}$ in figure 7 (see section 3.4.1 for the $\text{U}(1)^3$ knot-gauge theory $T[\mathbf{3_1}]$). The associated chiral fields are in table 5 and the associated Chern-Simons couplings are

$$k = -\frac{1}{2}, \quad k_c^{\text{g-f}} = \frac{3}{2}, \quad k^{\text{g-R}} = \frac{5}{2}, \quad k_c^{\text{f-R}} = 2. \qquad (4.4)$$
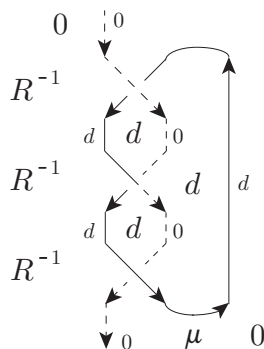
Figure 7. $(1,1)$-tangle diagram of the trefoil knot $\mathbf{3_1}$, where $0 \le d \le n$.

Field	U(1)	U(1)$_c$	mass	U(1)$_R$
$\Phi_1^{(1)}$	-1	1	γ_1	0
$\Phi_2^{(1)}$	0	0	γ_2	0
$\overline{\Phi}_3^{(1)}$	-1	0	γ_2^{-1}	2
$\overline{\Phi}_4^{(1)}$	0	-1	γ_1^{-1}	2
$\Phi_5^{(1)}$	1	0	1	0

Table 5. Matter content for the tangle diagram in figure 7, which corresponds to the R-matrix $\left(R^{-1}\right)^{d\,0}_{d\,0}$.

The gauge theory is considered to be a coupled system of the theories labeled by

$$T_1 = T[\overline{R}^{0\,d}_{d\,0}], \quad T_2 = T[\overline{R}^{d\,0}_{d\,0}(\boldsymbol{\gamma})], \quad T_3 = T[\overline{R}^{d\,0}_{0\,d}], \quad T_4 = T[\mu_d], \tag{4.5}$$

where the building block theory T_2 has mass parameters $\boldsymbol{\gamma} = (\gamma_1, \gamma_2)$ which are taken to be $\gamma_1, \gamma_2 \to 1$ at the end. The K-theoretic vortex partition function is given by[11]

$$I^{T^{\mathrm{red}}[\mathbf{3_1}]}_{\mathrm{vortex}}(\sigma; z, \boldsymbol{\gamma}, q) = \sum_d z^d \, I_n^{T_1}(q) \, I_n^{T_2}(\sigma; q) \, I_n^{T_3}(q) \, I_n^{T_4}(q). \tag{4.6}$$

Here z is the exponentiated FI parameter for the U(1) gauge symmetry that we take as $\xi = -\mathrm{Re}(\log z) > 0$, and the JK residue at $\sigma = \sigma^* = 1$ relevant to $\Phi_5^{(1)}$ is taken. Then, the K-theoretic vortex partition function (4.6) yields, by $z \to z^* = -1$ following (3.30) and $\boldsymbol{\gamma} \to \boldsymbol{\gamma}^* = (1,1)$, the normalized colored Jones polynomial of $\mathbf{3_1}$:

$$I^{T^{\mathrm{red}}[\mathbf{3_1}]}_{\mathrm{vortex}}(\sigma^*; z^*, \boldsymbol{\gamma}^*, q) = q^{\frac{3}{4}n(n+2)} \sum_{0 \le d \le n} \left(R^{-1}\right)^{0\,d}_{d\,0} \left(R^{-1}\right)^{d\,0}_{d\,0} \left(R^{-1}\right)^{d\,0}_{0\,d} \mu_d = J_n^{\mathbf{3_1}}(q)$$

$$= \sum_{0 \le d \le n} q^{(n+1)d+n} \frac{(q)_n}{(q)_{n-d}}. \tag{4.7}$$

It is easy to see that this result agrees with (3.59) with $f = 0$.

---

[11]In this section, for simplicity we use a notation $I_n^{T_i}(\boldsymbol{\sigma}; q) = I_{n,f=0}^{T_i}(\boldsymbol{\sigma}; q)$.
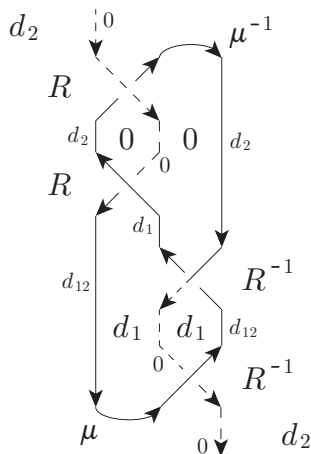
Figure 8. $(1,1)$-tangle diagram of the figure-eight knot $\mathbf{4_1}$, where $0 \leq d_2 \leq d_1 \leq n$.

Field	$U(1)_1$	$U(1)_2$	$U(1)_c$	mass	$U(1)_R$
$\Phi_1^{(1)}$	0	0	0	$\gamma_{1,1}$	0
$\Phi_2^{(1)}$	-1	0	1	$\gamma_{1,2}$	0
$\overline{\Phi}_3^{(1)}$	0	1	-1	$\gamma_{1,2}^{-1}$	2
$\overline{\Phi}_4^{(1)}$	-1	1	0	$\gamma_{1,1}^{-1}$	2
$\Phi_5^{(1)}$	1	-1	0	1	0
$\Phi_1^{(2)}$	0	-1	1	$\gamma_{2,1}$	0
$\Phi_2^{(2)}$	1	-1	0	$\gamma_{2,2}$	0
$\overline{\Phi}_3^{(2)}$	-1	0	0	$\gamma_{2,2}^{-1}$	2
$\overline{\Phi}_4^{(2)}$	0	0	-1	$\gamma_{2,1}^{-1}$	2
$\Phi_5^{(2)}$	0	1	0	1	0

Table 6. Matter content for the tangle diagram in figure 8, where the first (resp. second) table gives the R-matrix $R_{d_2 d_{12}}^{0\ \ d_1}$ (resp. $\left(R^{-1}\right)_{d_1\ 0}^{d_2 d_{12}}$).

4.2.2 Figure-eight knot 4_1

Consider a $(1,1)$-tangle diagram of the figure-eight knot $\mathbf{4_1}$ in figure 8. The reduced $U(1)^2$ knot-gauge theory $T^{\mathrm{red}}[\mathbf{4_1}]$ has the chiral fields in table 6 and Chern-Simons couplings

$$k_{11} = \frac{1}{2}, \quad k_{12} = k_{21} = -\frac{1}{2}, \quad k_{1c}^{\text{g-f}} = \frac{1}{2}, \quad k_{2c}^{\text{g-f}} = -1, \quad k_1^{\text{g-R}} = \frac{3}{2}, \quad k_2^{\text{g-R}} = -3, \quad (4.8)$$

and described as a coupled system of the theories labeled by

$$T_1 = T[R_{0\ \ d_2}^{d_2 0}], \qquad T_2 = T[R_{d_2 d_{12}}^{0\ \ d_1}(\gamma_{1,1}, \gamma_{1,2})], \qquad T_3 = T[\overline{R}_{d_1\ 0}^{d_2 d_{12}}(\gamma_{2,1}, \gamma_{2,2})],$$

$$T_4 = T[\overline{R}_{0\ \ d_{12}}^{d_{12} 0}], \qquad T_5 = T[\mu_{d_{12}}], \qquad T_6 = T[\overline{\mu}_{d_2}]. \qquad (4.9)$$

Here $d_{12} = d_1 - d_2$, and we note local deformations of tangle as

$$(4.10)$$

for the positive crossings and also for the negative crossings as well. Here mass parameters $\boldsymbol{\gamma} = (\gamma_{1,1}, \gamma_{1,2}, \gamma_{2,1}, \gamma_{2,2})$ are introduced for the building block theories T_2 and T_3. The K-theoretic vortex partition function is given by

$$I_{\text{vortex}}^{T^{\text{red}}[\mathbf{4_1}]}(\boldsymbol{\sigma}; \boldsymbol{z}, \boldsymbol{\gamma}, q) = \sum_{d_1, d_2} z_1^{d_1} z_2^{d_2} \prod_{i=1}^{6} I_n^{T_i}(\boldsymbol{\sigma}; q), \tag{4.11}$$

where $\boldsymbol{\sigma} = (\sigma_1, \sigma_2)$. Here $\boldsymbol{z} = (z_1, z_2)$ are the exponentiated FI parameters associated with the $\text{U}(1)_1 \times \text{U}(1)_2$ gauge symmetry, and for $\xi_i = -\text{Re}(\log z_i)$ we take (ξ_1, ξ_2) inside $\text{Cone}(Q_1, Q_2)$ which results in the JK residue at $\boldsymbol{\sigma} = \boldsymbol{\sigma}^* = (1,1)$, where $Q_1 = (1, -1)$ and $Q_2 = (0, 1)$ are charge vectors of $\Phi_5^{(1)}$ and $\Phi_5^{(2)}$, respectively. As a result, by $\boldsymbol{z} \to \boldsymbol{z}^* = (-1, -1)$ following (3.20) and (3.30), and $\boldsymbol{\gamma} \to \boldsymbol{\gamma}^*$ with $\gamma_{1,1}^* = \gamma_{1,2}^* = \gamma_{2,1}^* = \gamma_{2,2}^* = 1$, the K-theoretic vortex partition function (4.11) yields the normalized colored Jones polynomial of $\mathbf{4_1}$:

$$I_{\text{vortex}}^{T^{\text{red}}[\mathbf{4_1}]}(\boldsymbol{\sigma}^*; \boldsymbol{z}^*, \boldsymbol{\gamma}^*, q)$$

$$= \sum_{0 \le d_2 \le d_1 \le n} R^{d_2 0}_{0 \ d_2} R^{0 \ d_1}_{d_2 d_{12}} \left(R^{-1} \right)^{d_2 d_{12}}_{d_1 \ 0} \left(R^{-1} \right)^{d_{12} 0}_{0 \ d_{12}} \mu_{d_{12}} \mu_{d_2}^{-1}$$

$$= J_n^{\mathbf{4_1}}(q)$$

$$= \sum_{0 \le d_2 \le d_1 \le n} (-1)^{d_1 + d_2} q^{\frac{1}{2} d_2 (d_2 - 2d_1 - 2n - 3) + \frac{1}{2} d_1 (d_1 + 1)} \frac{(q)_{d_1} (q)_n}{(q)_{d_2} (q)_{d_{12}} (q)_{n - d_1}}. \tag{4.12}$$

Remark 4.1. By a formula [45, Lemma A.1]

$$\sum_{0 \le d \le k} (-1)^d q^{\frac{1}{2} d (d + \ell)} \frac{(q)_k}{(q)_d (q)_{k-d}} = \left(q^{\frac{1}{2}(\ell+1)}; q \right)_k = (-1)^k q^{\frac{1}{2} k (k + \ell)} \left(q^{\frac{1}{2}(1 - \ell - 2k)}; q \right)_k, \tag{4.13}$$

which follows from the q-Pascal relation (3.64), the colored Jones polynomial (4.12) is written by a single sum as [55–57]

$$J_n^{\mathbf{4_1}}(q) = \sum_{0 \le d_1 \le n} q^{-(n+1) d_1} \left(q^{n+2}; q \right)_{d_1} \left(q^{n - d_1 + 1}; q \right)_{d_1}. \tag{4.14}$$

4.2.3 3-twist knot $\mathbf{5_2}$

Consider the reduced $\text{U}(1)^3$ knot-gauge theory $T^{\text{red}}[\mathbf{5_2}]$ associated with a $(1,1)$-tangle diagram of the 3-twist knot $\mathbf{5_2}$ in figure 9. The chiral fields are in table 7, and by noting the local deformations (4.10) the non-zero Chern-Simons couplings are given by

$$k_{11} = k_{12} = k_{21} = -\frac{1}{2}, \quad k_{22} = 1, \quad k_{33} = k_{13} = k_{31} = \frac{1}{2}, \quad k_{23} = k_{32} = -1,$$

$$k_{1c}^{\text{g-f}} = \frac{3}{2}, \quad k_{2c}^{\text{g-f}} = 1, \quad k_{3c}^{\text{g-f}} = -\frac{3}{2}, \quad k_1^{\text{g-R}} = \frac{3}{2}, \quad k_2^{\text{g-R}} = 1, \quad k_3^{\text{g-R}} = -\frac{7}{2}, \quad k_c^{\text{f-R}} = 4. \tag{4.15}$$
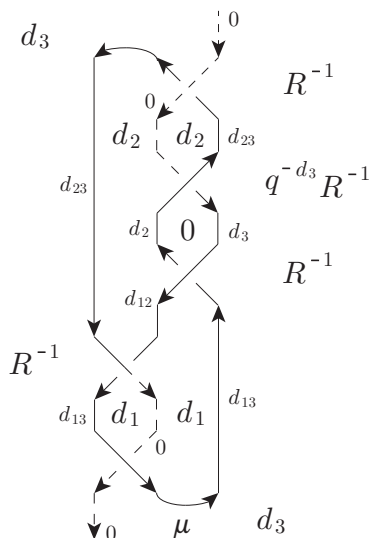
Figure 9. $(1,1)$-tangle diagram of the 3-twist knot $\mathbf{5_2}$, where $0 \leq d_{12} \leq d_3 \leq d_2 \leq n$.

Field	$U(1)_1$	$U(1)_2$	$U(1)_3$	$U(1)_c$	mass	$U(1)_R$
$\Phi_1^{(1)}$	0	-1	0	1	$\gamma_{1,1}$	0
$\Phi_2^{(1)}$	0	0	0	0	$\gamma_{1,2}$	0
$\overline{\Phi}_3^{(1)}$	0	0	-1	0	$\gamma_{1,2}^{-1}$	2
$\overline{\Phi}_4^{(1)}$	0	1	-1	-1	$\gamma_{1,1}^{-1}$	2
$\Phi_5^{(1)}$	0	0	1	0	1	0
$\Phi_1^{(2)}$	0	0	-1	1	$\gamma_{2,1}$	0
$\Phi_2^{(2)}$	1	0	-1	0	$\gamma_{2,2}$	0
$\overline{\Phi}_3^{(2)}$	0	-1	0	0	$\gamma_{2,2}^{-1}$	2
$\overline{\Phi}_4^{(2)}$	1	-1	0	-1	$\gamma_{2,1}^{-1}$	2
$\Phi_5^{(2)}$	-1	1	1	0	1	0
$\Phi_1^{(3)}$	0	-1	1	1	$\gamma_{3,1}$	0
$\Phi_2^{(3)}$	1	-1	0	0	$\gamma_{3,2}$	0
$\overline{\Phi}_3^{(3)}$	-1	0	1	0	$\gamma_{3,2}^{-1}$	2
$\overline{\Phi}_4^{(3)}$	0	0	0	-1	$\gamma_{3,1}^{-1}$	2
$\Phi_5^{(3)}$	0	1	-1	0	1	0

Table 7. Matter content for the tangle diagram in figure 9, where the first, second and third tables correspond to the inverse R-matrices $\left(R^{-1}\right)_{d_3 d_{23}}^{d_2 0}$, $\left(R^{-1}\right)_{d_2 d_{12}}^{d_3 d_{13}}$ and $\left(R^{-1}\right)_{d_{13} 0}^{d_{23} d_{12}}$, respectively.

The gauge theory is a coupled system of the theories labeled by

$$
\begin{aligned}
&T_1 = T[\overline{R}_{d_{23} 0}^{0\ d_{23}}], && T_2 = T[\overline{R}_{d_3 d_{23}}^{d_2 0}(\gamma_{1,1}, \gamma_{1,2})], && T_3 = T[\overline{R}_{d_2 d_{12}}^{d_3 d_{13}}(\gamma_{2,1}, \gamma_{2,2})], \\
&T_4 = T[\overline{R}_{d_{13} 0}^{d_{23} d_{12}}(\gamma_{3,1}, \gamma_{3,2})], && T_5 = T[\overline{R}_{0\ d_{13}}^{d_{13} 0}], \\
&T_6 = T[\mu_{d_{13}}], && T_7 = T[\mu_{d_{23}}], && T_8 = T[\overline{\mu}_{d_2}], && (4.16)
\end{aligned}
$$

where $d_{ij} = d_i - d_j$, and mass parameters $\boldsymbol{\gamma} = (\gamma_{1,1}, \gamma_{1,2}, \gamma_{2,1}, \gamma_{2,2}, \gamma_{3,1}, \gamma_{3,2})$ are introduced in the building block theories T_2, T_3 and T_4. The K-theoretic vortex partition function is given by

$$I_{\text{vortex}}^{T^{\text{red}}[\mathbf{5_2}]}(\boldsymbol{\sigma}; \boldsymbol{z}, \boldsymbol{\gamma}, q) = \sum_{d_1, d_2, d_3} z_1^{d_1} z_2^{d_2} z_3^{d_3} \prod_{i=1}^{8} I_n^{T_i}(\boldsymbol{\sigma}; q), \tag{4.17}$$

where $\boldsymbol{\sigma} = (\sigma_1, \sigma_2, \sigma_3)$. Here $\boldsymbol{z} = (z_1, z_2, z_3)$ are the exponentiated FI parameters for the $\text{U}(1)_1 \times \text{U}(1)_2 \times \text{U}(1)_3$ gauge symmetry, and for $\xi_i = -\text{Re}(\log z_i)$ we take (ξ_1, ξ_2, ξ_3) inside $\text{Cone}(Q_1, Q_2, Q_3)$ so that only the JK residue at $\boldsymbol{\sigma} = \boldsymbol{\sigma}^* = (1, 1, 1)$ finally contributes, where $Q_1 = (0, 0, 1)$, $Q_2 = (-1, 1, 1)$, and $Q_3 = (0, 1, -1)$ are the charge vectors of $\Phi_5^{(1)}$, $\Phi_5^{(2)}$, and $\Phi_5^{(3)}$, respectively. The K-theoretic vortex partition function (4.17) then yields, by $\boldsymbol{z} \to \boldsymbol{z}^* = (1, -1, -1)$ following (3.30) and $\boldsymbol{\gamma} \to \boldsymbol{\gamma}^*$ with $\gamma_{k,\ell}^* = 1$, the normalized colored Jones polynomial of $\mathbf{5_2}$:

$$\begin{aligned}
I_{\text{vortex}}^{T^{\text{red}}[\mathbf{5_2}]}(\boldsymbol{\sigma}^*; \boldsymbol{z}^*, \boldsymbol{\gamma}^*, q) &= q^{\frac{5}{4}n(n+2)} \sum_{0 \le d_{12} \le d_3 \le d_2 \le n} q^{-d_3} \left(R^{-1}\right)_{d_{23}0}^{0\ d_{23}} \left(R^{-1}\right)_{d_3 d_{23}}^{d_2 0} \\
&\qquad \times \left(R^{-1}\right)_{d_2 d_{12}}^{d_3 d_{13}} \left(R^{-1}\right)_{d_{13}0}^{d_{23} d_{12}} \left(R^{-1}\right)_{0\ d_{13}}^{d_{13} 0} \mu_{d_{13}} \\
&= J_n^{\mathbf{5_2}}(q) \\
&= \sum_{0 \le d_{12} \le d_3 \le d_2 \le n} q^{-d_{12}d_2 - d_3 d_{23} + 2n(d_{12} + d_{23}) + d_{12} + d_2 - 2d_3 + 2n} \\
&\qquad \times \frac{(q)_{d_2} (q)_{n-d_{12}} (q)_n}{(q)_{n-d_2} (q)_{n-d_3} (q)_{d_3 - d_{12}} (q)_{d_{23}} (q)_{d_{12}}}. \tag{4.18}
\end{aligned}$$

Acknowledgments

A q-Pochhammer symbol

The q-Pochhammer symbol is defined by

$$(x; q)_d = \frac{(x; q)_\infty}{(xq^d; q)_\infty} = \begin{cases} \prod_{k=0}^{d-1} \left(1 - xq^k\right) & \text{if } d \in \mathbb{Z}_{>0}, \\ 1 & \text{if } d = 0, \\ \prod_{k=d}^{-1} \left(1 - xq^k\right)^{-1} & \text{if } d \in \mathbb{Z}_{<0}. \end{cases} \tag{A.1}$$

The q-Pochhammer symbol has the following properties:

$$\begin{aligned}
(x; q)_d &= \left(q^{d-1} x; q^{-1}\right)_d = (-x)^d q^{\frac{1}{2}d(d-1)} \left(x^{-1}; q^{-1}\right)_d \\
&= (-x)^d q^{\frac{1}{2}d(d-1)} \left(q^{-d+1} x^{-1}; q\right)_d = \left(q^d x; q\right)_{-d}^{-1}
\end{aligned}$$

$$= \left(q^{-1}x; q^{-1} \right)_{-d}^{-1} = (-x)^d q^{\frac{1}{2}d(d-1)} \left(qx^{-1}; q \right)_{-d}^{-1}, \tag{A.2}$$

$$(x; q)_{d_1+d_2} = (x; q)_{d_1} \left(q^{d_1}x; q \right)_{d_2} = \frac{(x; q)_{d_1}}{(q^{d_1+d_2}x; q)_{-d_2}} = \frac{\left(q^{d_2}x; q \right)_{d_1}}{(q^{d_2}x; q)_{-d_2}}, \tag{A.3}$$

for any $d, d_1, d_2 \in \mathbb{Z}$ and a generic $x \in \mathbb{C}$. We also use a notation $(q)_d = (q; q)_d$ when $x = q$.

Open Access. This article is distributed under the terms of the Creative Commons Attribution License ([CC-BY 4.0](#)), which permits any use, distribution and reproduction in any medium, provided the original author(s) and source are credited.

References

[1] V. Pestun et al., *Localization techniques in quantum field theories*, *J. Phys. A* **50** (2017) 440301 [`arXiv:1608.02952`] [INSPIRE].

[2] F. Benini and A. Zaffaroni, *A topologically twisted index for three-dimensional supersymmetric theories*, *JHEP* **07** (2015) 127 [`arXiv:1504.03698`] [INSPIRE].

[3] S. Pasquetti, *Factorisation of N = 2 theories on the squashed 3-sphere*, *JHEP* **04** (2012) 120 [`arXiv:1111.6905`] [INSPIRE].

[4] T. Dimofte, D. Gaiotto and S. Gukov, *3-manifolds and 3d indices*, *Adv. Theor. Math. Phys.* **17** (2013) 975 [`arXiv:1112.5179`] [INSPIRE].

[5] C. Beem, T. Dimofte and S. Pasquetti, *Holomorphic blocks in three dimensions*, *JHEP* **12** (2014) 177 [`arXiv:1211.1986`] [INSPIRE].

[6] S. Cecotti, D. Gaiotto and C. Vafa, *tt* geometry in 3 and 4 dimensions*, *JHEP* **05** (2014) 055 [`arXiv:1312.1008`] [INSPIRE].

[7] M. Fujitsuka, M. Honda and Y. Yoshida, *Higgs branch localization of 3d N = 2 theories*, *PTEP* **2014** (2014) 123B02 [`arXiv:1312.3627`] [INSPIRE].

[8] F. Benini and W. Peelaers, *Higgs branch localization in three dimensions*, *JHEP* **05** (2014) 030 [`arXiv:1312.6078`] [INSPIRE].

[9] F. Nieri and S. Pasquetti, *Factorisation and holomorphic blocks in 4d*, *JHEP* **11** (2015) 155 [`arXiv:1507.00261`] [INSPIRE].

[10] C. Hwang, P. Yi and Y. Yoshida, *Fundamental vortices, Wall-Crossing, and particle-vortex duality*, *JHEP* **05** (2017) 099 [`arXiv:1703.00213`] [INSPIRE].

[11] S. Crew, N. Dorey and D. Zhang, *Factorisation of 3d N = 4 twisted indices and the geometry of vortex moduli space*, *JHEP* **08** (2020) 015 [`arXiv:2002.04573`] [INSPIRE].

[12] E. Witten, *Quantum field theory and the Jones polynomial*, *Commun. Math. Phys.* **121** (1989) 351 [INSPIRE].

[13] Y. Terashima and M. Yamazaki, SL(2, R) *Chern-Simons, Liouville, and gauge theory on duality walls*, *JHEP* **08** (2011) 135 [`arXiv:1103.5748`] [INSPIRE].

[14] Y. Terashima and M. Yamazaki, *Semiclassical analysis of the 3d/3d relation*, *Phys. Rev. D* **88** (2013) 026011 [`arXiv:1106.3066`] [INSPIRE].

[15] T. Dimofte and S. Gukov, *Chern-Simons theory and S-duality*, *JHEP* **05** (2013) 109 [`arXiv:1106.4550`] [INSPIRE].

[16] T. Dimofte, D. Gaiotto and S. Gukov, *Gauge theories labelled by three-manifolds*, *Commun. Math. Phys.* **325** (2014) 367 [arXiv:1108.4389] [InSPIRE].

[17] S. Cecotti, C. Cordova and C. Vafa, *Braids, walls, and mirrors*, arXiv:1110.2115 [InSPIRE].

[18] H. Fuji, S. Gukov, M. Stosic and P. Sulkowski, *3d analogs of Argyres-Douglas theories and knot homologies*, *JHEP* **01** (2013) 175 [arXiv:1209.1416] [InSPIRE].

[19] H.-J. Chung, T. Dimofte, S. Gukov and P. Sułkowski, *3d-3d correspondence revisited*, *JHEP* **04** (2016) 140 [arXiv:1405.3663] [InSPIRE].

[20] T. Dimofte, S. Gukov and L. Hollands, *Vortex counting and Lagrangian 3-manifolds*, *Lett. Math. Phys.* **98** (2011) 225 [arXiv:1006.0977] [InSPIRE].

[21] D. Gaiotto, *N = 2 dualities*, *JHEP* **08** (2012) 034 [arXiv:0904.2715] [InSPIRE].

[22] L.F. Alday, D. Gaiotto and Y. Tachikawa, *Liouville correlation functions from four-dimensional gauge theories*, *Lett. Math. Phys.* **91** (2010) 167 [arXiv:0906.3219] [InSPIRE].

[23] V.G. Turaev, *The Yang-Baxter equation and invariants of links*, *Invent. Math.* **92** (1988) 527.

[24] H. Murakami, *An introduction to the volume conjecture*, arXiv:1002.0126.

[25] L.C. Jeffrey and F.C. Kirwan, *Localization for nonabelian group actions*, *Topology* **34** (1995) 291 [alg-geom/9307001].

[26] M. Brion and M. Vergne, *Arrangements of hyperplanes I: rational functions and Jeffrey-Kirwan residue*, *Ann. Sci. Ecole Norm. Sup.* **32** (1999) 715 [math.DG/9903178].

[27] A. Szenes and M. Vergne, *Toric reduction and a conjecture of Batyrev and Materov*, *Invent. Math.* **158** (2004) 453 [math.AT/0306311].

[28] F. Benini, R. Eager, K. Hori and Y. Tachikawa, *Elliptic genera of 2d $\mathcal{N} = 2$ gauge theories*, *Commun. Math. Phys.* **333** (2015) 1241 [arXiv:1308.4896] [InSPIRE].

[29] M. Bullimore and A. Ferrari, *Twisted Hilbert spaces of 3d supersymmetric gauge theories*, *JHEP* **08** (2018) 018 [arXiv:1802.10120] [InSPIRE].

[30] M. Bullimore, A. Ferrari and H. Kim, *Twisted indices of 3d $\mathcal{N} = 4$ gauge theories and enumerative geometry of quasi-maps*, *JHEP* **07** (2019) 014 [arXiv:1812.05567] [InSPIRE].

[31] S. Kim, *The Complete superconformal index for $N = 6$ Chern-Simons theory*, *Nucl. Phys. B* **821** (2009) 241 [*Erratum ibid.* **864** (2012) 884] [arXiv:0903.4172] [InSPIRE].

[32] Y. Imamura and S. Yokoyama, *Index for three dimensional superconformal field theories with general R-charge assignments*, *JHEP* **04** (2011) 007 [arXiv:1101.0557] [InSPIRE].

[33] A. Kapustin and B. Willett, *Generalized superconformal index for three dimensional field theories*, arXiv:1106.2484 [InSPIRE].

[34] M. Bullimore, A.E.V. Ferrari, H. Kim and G. Xu, *The twisted index and topological saddles*, arXiv:2007.11603 [InSPIRE].

[35] F. Benini and A. Zaffaroni, *Supersymmetric partition functions on Riemann surfaces*, *Proc. Symp. Pure Math.* **96** (2017) 13 [arXiv:1605.06120] [InSPIRE].

[36] C. Closset and H. Kim, *Comments on twisted indices in 3d supersymmetric gauge theories*, *JHEP* **08** (2016) 059 [arXiv:1605.06531] [InSPIRE].

[37] K. Ueda and Y. Yoshida, *3d $\mathcal{N} = 2$ Chern-Simons-matter theory, Bethe ansatz, and quantum K-theory of Grassmannians*, *JHEP* **08** (2020) 157 [arXiv:1912.03792] [InSPIRE].

[38] Y. Yoshida and K. Sugiyama, *Localization of three-dimensional $\mathcal{N} = 2$ supersymmetric theories on $S^1 \times D^2$*, *PTEP* **2020** (2020) 113B02 [`arXiv:1409.6713`] [INSPIRE].

[39] S. Crew, N. Dorey and D. Zhang, *Blocks and vortices in the 3d ADHM quiver gauge theory*, *JHEP* **03** (2021) 234 [`arXiv:2010.09732`] [INSPIRE].

[40] M. Bullimore, S. Crew and D. Zhang, *Boundaries, vermas, and factorisation*, *JHEP* **04** (2021) 263 [`arXiv:2010.09741`] [INSPIRE].

[41] R. Kirby and P. Melvin, *The 3-manifold invariants of Witten and Reshetikhin-Turaev for $sl(2, C)$*, *Invent. Math.* **105** (1991) 473.

[42] J. Cho and J. Murakami, *Optimistic limits of the colored Jones polynomials*, *Bull. Korean Math. Soc.* **50** (2013) 641 [`arXiv:1009.3137`].

[43] D. Thurston, *Hyperbolic volume and the Jones polynomial*, lecture note at *Invariants des noeuds et de variétés de dimension 3* (1999), available at https://dpthurst.pages.iu.edu/speaking/Grenoble.pdf.

[44] R.M. Kashaev, *The Hyperbolic volume of knots from quantum dilogarithm*, *Lett. Math. Phys.* **39** (1997) 269 [INSPIRE].

[45] H. Murakami and J. Murakami, *The colored Jones polynomials and the simplicial volume of a knot*, *Acta Math.* **186** (2001) 85 [`math.GT/9905075`].

[46] Y. Yokota, *On the complex volume of hyperbolic knots*, *J. Knot Theory Ramif.* **20** (2011) 955.

[47] H. Murakami, *Kashaev's invariant and the volume of a hyperbolic knot after Y. Yokota*, *Phys. Combin.* (2001) 244 [`math.GT/0008027`].

[48] P. Kucharski, M. Reineke, M. Stosic and P. Sułkowski, *BPS states, knots and quivers*, *Phys. Rev. D* **96** (2017) 121902 [`arXiv:1707.02991`] [INSPIRE].

[49] P. Kucharski, M. Reineke, M. Stosic and P. Sułkowski, *Knots-quivers correspondence*, *Adv. Theor. Math. Phys.* **23** (2019) 1849 [`arXiv:1707.04017`] [INSPIRE].

[50] T. Ekholm, P. Kucharski and P. Longhi, *Physics and geometry of knots-quivers correspondence*, *Commun. Math. Phys.* **379** (2020) 361 [`arXiv:1811.03110`] [INSPIRE].

[51] T. Ekholm, P. Kucharski and P. Longhi, *Multi-cover skeins, quivers, and 3d $\mathcal{N} = 2$ dualities*, *JHEP* **02** (2020) 018 [`arXiv:1910.06193`] [INSPIRE].

[52] J. Jankowski, P. Kucharski, H. Larraguível, D. Noshchenko and P. Sułkowski, *Permutohedra for knots and quivers*, *Phys. Rev. D* **104** (2021) 086017 [`arXiv:2105.11806`] [INSPIRE].

[53] T. Ekholm, P. Kucharski and P. Longhi, *Knot homologies and generalized quiver partition functions*, `arXiv:2108.12645` [INSPIRE].

[54] A. Gorsky, A. Milekhin and N. Sopenko, *The condensate from torus knots*, *JHEP* **09** (2015) 102 [`arXiv:1506.06695`] [INSPIRE].

[55] H. Murakami, *The asymptotic behavior of the colored Jones function of a knot and its volume*, `math.GT/0004036`.

[56] T.T.Q. Le, *Quantum invariants of 3-manifolds: integrality, splitting, and perturbative expansion*, *Topol. Appl.* **127** (2003) 125 [`math.QA/0004099`].

[57] K. Habiro, *On the quantum sl_2 invariants of knots and integral homology spheres*, *Geom. Topol. Monogr.* **4** (2002) 55 [`math.GT/0211044`].